THE LIMITS OF BRUNE'S IMPEDANCE

BY

ROGER DAVID SERWY

THESIS

Submitted in partial fulfillment of the requirements
for the degree of Master of Science in Electrical and Computer Engineering
in the Graduate College of the
University of Illinois at Urbana-Champaign, 2012

Urbana, Illinois

Adviser:

Associate Professor Jont B. Allen

ABSTRACT

The impedance concept as popularized by Oliver Heaviside in the 1880s may be used to model physical systems that may or may not include wave propagation. Otto Brune in 1931 coined the term and then provided a proof that "positive real" is a necessary and sufficient condition for network synthesis using lumped elements. Brune's impedance, described using a ratio of polynomials, represents a fundamentally limited subset of impedance functions. Quite notably, all lumped-element networks do not support wave propagation.

Two classes of impedances emerge in this analysis, the c-finite and c-infinite. These two classes separate the physical assumption of wave propagation used in modeling an impedance structure. The c-infinite class deals with impedances where the speed of wave propagation is infinite and, as a consequence, describes simultaneous systems. The c-finite class describes systems with a finite wave speed, and thus describes non-simultaneous systems.

These two classes have unique mathematical properties in both the time and frequency domains. Unfortunately, the traditional approach to impedance as an exclusive frequency-domain concept hides the distinction between the c-finite and c-infinite impedance classes. This thesis will explore these two classes, as well as how both classes can approximate each other.

The c-finite impedance class offers an alternative way of formulating Ohm's law in the time domain by means of a reflectance, a special Möbius transformation of the impedance formula. Reflectance offers an alternative means of expressing Ohm's law by means of wave propagation. This Möbius transformation also allows for a reformulation of positive real (PR), which is used to develop a test for the PR property of a rational function.

To my parents, for their love and support

TABLE OF CONTENTS

LIST OF TABLES vi

LIST OF FIGURES vii

LIST OF ABBREVIATIONS ix

CHAPTER 1 INTRODUCTION 1
1.1 Basic Results 2
1.2 Resistance in the Time and Frequency Domains 3
1.3 History of Impedance 4
1.4 Organization of This Thesis 5
1.5 Motivation 6

CHAPTER 2 NETWORK ANALYSIS AND LUMPED ELEMENTS 7
2.1 Quasistatic Approximations 8
2.2 Pole and Zero Locations 9

CHAPTER 3 THE BRUNE IMPEDANCE 11
3.1 Positive Real 11
3.2 Example Circuit 13
3.3 Toward a Time-Domain Expression 14

CHAPTER 4 TRANSMISSION LINE IMPEDANCES 18
4.1 Time-Domain Properties of C-Finite Impedance 19
4.2 Uniform Transmission Line Parameters 21
4.3 Line as a C-Finite Impedance 21
4.4 Line as a C-Infinite Impedance 22
4.5 Pure Loss (Resistor) 23
4.6 Loaded Transmission Lines 24
4.7 Branch Cuts and Positive Real 25

CHAPTER 5 THE BILINEAR TRANSFORM AND DISCRETE-TIME IMPEDANCE 26
5.1 Discrete-Time Impedance 26

5.2 Stub Approximations 27
5.3 Input Impedance to Elements 29
5.4 Discrete Realization 31

CHAPTER 6 THE C-INFINITE AND C-FINITE IMPEDANCE CLASSES 33
6.1 The C-Finite Class 33
6.2 Rational Function Impedances as C-Finite 34
6.3 The C-Infinite class 37
6.4 Frequency Domain Manipulation 38
6.5 Interlinking C-Infinite and C-Finite 40
6.6 The Non-simultaneous Universe 42
6.7 SPICE and C-Finite 42

CHAPTER 7 THE MÖBIUS TRANSFORM AND POSITIVE REAL 44
7.1 Möbius Transform 44
7.2 Positive Real for a Möbius-Transformed Impedance 46
7.3 Testing for Positive Real 47
7.4 Factoring a Möbius-Transformed Impedance 48
7.5 Poles and Zeros of RLC Impedance Networks 53

CHAPTER 8 REFLECTANCE AND THE REFLECTION COEFFICIENT 55
8.1 Reflection Coefficient 55
8.2 Reflectance 56
8.3 Reflectance Signal Flow Diagram 58
8.4 Physical Interpretation of Reflectance 58
8.5 Contrasting the Reflectance with the Reflection Coefficient . . 59
8.6 Reflectance Examples 60

CHAPTER 9 CONCLUSIONS 66

APPENDIX A THE LAPLACE TRANSFORM 70
A.1 Initial Singularity Theorem 70
A.2 Initial Value Theorem 71
A.3 Laplace Transform Identities 71

APPENDIX B NON-UNIFORM TRANSMISSION LINES 73
B.1 Spherical Radiator Derivation 73
B.2 Webster Horn Equation 74
B.3 Acoustic Capacitors 75
B.4 Salmon Family of Horns 76

REFERENCES 79

LIST OF TABLES

2.1 Lumped-element assumptions for an inductor, capacitor, and resistor. 9

A.1 Table of select inverse Laplace transform identities from Campbell and Foster (1942). 72

B.1 Equivalent variables between electrical and acoustical formulation. 75

LIST OF FIGURES

2.1 Example placement of poles and zeros for an LC network. . . 10
2.2 Example placement of poles and zeros for an RC and RL network. 10

3.1 Real and imaginary parts of Eq. 3.2. 14
3.2 Magnitude and phase of Eq. 3.2. 15

5.1 A short transmission line stub network. 27
5.2 TX line stub and ideal component impedances. 28
5.3 Signal flow diagram for implementing Ohm's law for a discrete-time capacitor $z_C(t)$. 31
5.4 Signal flow diagram for implementing Ohm's law for a discrete-time inductor $z_L(t)$. 32

6.1 Reproductions of Figs. 2 and 5 from Parent and Allen (2007). 39
6.2 A depiction of the Padé approximation and its relation to the Taylor series. 41

7.1 Resultant network when factoring the Möbius-transformed impedance expression using a unity gyrator, indicated by the dashed border. 51
7.2 Impedance network will all elements of unity value: 1, s, 1/s 52

8.1 Incident and reflected waves at a boundary for describing a reflection coefficient. 56
8.2 Incident and reflected waves at an ideal current source for describing the reflectance of the c-finite impedance $Z(s)$. . . . 57
8.3 Signal flow diagram for a reflectance in Fig. 8.2 and the time domain Eq. 8.15. 58
8.4 Approximations to $e^{-\sigma}$ following Eqs. 8.24 to 8.26 62
8.5 Padé approximation to e^{-s} and pole/zero pattern. This is a valid reflectance. 63

8.6 Padé approximation to e^{-s} and all-pass pole/zero pattern. This is not a valid reflectance due to its initial time-domain singularity. 64

B.1 Radii and impedance of equi-volume cavities. 77
B.2 Salmon family of horns. Real components of Z and $\mathcal{G}$ are solid lines; imaginary components are dashed lines. 78

LIST OF ABBREVIATIONS

PR	Positive real
LHP	Left-half plane (complex s plane)
RHP	Right-half plane (complex s plane)
IIR	Infinite impulse response
MP	Minimum phase
$\Re$	Real component
$\Im$	Imaginary component
$\mathcal{L}^{-1}$	Inverse Laplace transform
s	Complex frequency ($\sigma + j\omega$) [radians]
$u(t)$	Heaviside unit step function
Z	Impedance [Ohms]
R	Resistance [Ohms] or [Ohms/meter]
L	Inductance [Henries] or [Henries/meter]
C	Capacitance [Farads] or [Farads/meter]
G	Conductance [Siemens] or [Siemens/meter]
R_0	Real surge impedance [Ohms]
R_m	Positive Möbius transformation constant
$M(s)$	Möbius-transformed impedance
$\Gamma(s)$	Reflection coefficient
$\mathcal{G}(s)$, $g(t)$	Reflectance

c	Speed of wave propagation [meters/second]
T	Delay (propagation or period) [second]
$\mathfrak{L}$	Length of a transmission line [meters]

CHAPTER 1

INTRODUCTION

Otto Brune first described the mathematical properties of an impedance, known as *positive real*, that guarantee a network representation using lumped elements. The rational function formulation Brune described, while very useful, has fundamental limitations. These impedances describe simultaneous networks that require solutions to simultaneous equations, whereas the physical world is not simultaneous. This thesis explores a more general approach toward impedance modeling that considers non-simultaneity and how it relates to Brune's formulation.

Impedance is a model of a physical system, and as such can require certain physical assumptions. Two fundamental classes of impedance emerge, *c-infinite* and *c-finite*, and involve how the impedance model incorporates wave propagation. The c-infinite class describes lumped element networks as well as distributed systems without wave propagation. These systems are effectively simultaneous and require solutions to simultaneous equations. The c-finite class describes impedances of a wave-propagating device, e.g. transmission lines, which are inherently non-simultaneous and thus can be solved recursively. These two separate impedance classes have several unique frequency and time domain properties, despite sometimes sharing a similar mathematical form.

A closely related concept to impedance is *reflectance*. Based on a purely mathematical formulation, reflectance offers an alternative method for expressing the relationship between current and voltage with its own set of mathematical properties. Reflectance has a very physical interpretation for c-finite impedances since the underlying system must contain wave propagation. Forward and backward traveling waves in the impedance structure combine to represent voltage and current at the input, and the ratio of these waves defines the reflectance. Reflectance also has an abstract mathematical interpretation for c-infinite impedances but lacks the strict

physical interpretation of wave propagation.

The reflectance concept will also be contrasted against the one-port scattering parameter, commonly known as a *reflection coefficient*. Reflectance, as defined in this thesis, is a property of a one-port c-finite impedance itself and does not require a source impedance. This subtle distinction allows for a different perspective on the nature of impedance through interpreting its reflectance.

Many example systems will be discussed and explained from the context of impedance and reflectance.

1.1 Basic Results

Two impedance classes emerge: c-finite and c-infinite. These classes are not immediately apparent when working strictly in the frequency domain, but do become obvious when considering the time-domain properties of impedance.

All c-finite impedances have the following time-domain form:

$$z(t) = R_0\delta(t) + z_{res}(t)\,u(t) \tag{1.1}$$

where R_0 represents the initial surge impedance of a wave initially entering into the impedance structure and $z_{res}(t)u(t)$ representing the causal residual, "reactive" waves reflecting back to the input. The c-finite class includes transmission lines and radiation impedances.

The c-infinite class contains quasistatic lumped elements as well as distributed systems that do not support wave propagation, such as diffusion lines. The c-infinite impedance class, due to its physical modeling, does not have wave propagation and as a result may have a very different time-domain formulation from c-finite impedances.

Each of these two impedance class can approximate the other by various means, such as by applying a bilinear transformation or performing a Padé approximation

Certain lumped-element models may share the time-domain expression of a c-finite impedance, given in Eq. 1.1. This means that the c-infinite impedance has an equivalent expression as a c-finite transmission line impedance. In such cases, the spatial properties of this transmission line may be derived

exactly from the time-domain input impedance formula by means of Sondhi and Gopinath's inverse solution (Sondhi & Gopinath, 1971).

A Möbius transformation of a c-finite impedance gives a function which offers a unique time-domain representation of Ohm's law, distinct from a purely convolutional relationship. The properties of positive real have a simpler realization in this Möbius-transformed impedance domain. A test procedure for determining if a rational function satisfies PR is given.

1.2 Resistance in the Time and Frequency Domains

The simple resistor can serve as a simple motivator into exploring the time- and frequency-domain properties of an impedance. The frequency-domain expression for a resistor is a real constant, *independent of frequency*:

$$Z(s) = R \tag{1.2}$$

Its time-domain expression, by means of an inverse Laplace transform, is given as:

$$z(t) = R\,\delta(t) \tag{1.3}$$

Ohm's law is a multiplicative relationship in the frequency domain, meaning that it is a *convolutional* relationship in the time domain, shown in Eq. 1.4.

$$V(s) = I(s)Z(s) \quad \overset{\mathcal{L}^{-1}}{\longleftrightarrow} \quad v(t) = \int_{0-}^{t} i(\tau)z(t-\tau)d\tau \tag{1.4}$$

Placing the time-domain impedance for a resistor in the convolution yields:

$$v(t) = i(t)R \tag{1.5}$$

due to the "sifting" property of the Dirac delta function. The time-domain resistor is a degenerate case within Ohm's law since it hides its true convolutional relationship.

This simple example of the resistor's behavior in the time and frequency domain may seem trivial, as it is. It does, however, offer some insight into thinking about impedance in both the time and frequency domains. This notion will become increasingly important as more complicated impedances

are considered.

The realization of the resistor can become much more complicated as will be shown in Section 4.5.

1.3 History of Impedance

The impedance concept begins with Georg Ohm in 1827 who published the now famous result $V = IR$. This was a time-domain expression relating DC voltage and current. A few decades later in 1847, Gustav Kirchhoff published his circuit interconnection laws, commonly known as Kirchhoff's current (KCL) and voltage (KVL) laws. James Clerk Maxwell, building on the results of Ampere and Faraday, unified the observations of electrical, magnetic, and optical phenomena as electromagnetism in his famous 1865 treatise.

Oliver Heaviside, a telegrapher and nephew of Charles Wheatstone, reformulated Maxwell's equation using vector analysis, providing the four equations commonly used to this day. Heaviside also developed operational calculus and the telegrapher's equations for describing the behavior of electrical circuits. The terms "impedance" and "reactance" were coined by Heaviside for describing the properties emerging from his operational calculus formulations (Heaviside, 1950).

With the invention of the telephone, much research went into understanding electrical circuits. George Campbell developed the electric wave filter in 1910, a cornerstone of modern analog filter theory. Developing circuits with certain prescribed properties led to the field of network synthesis where Wilhelm Cauer provided much of its early mathematical foundation. Ronald Foster provided a theorem and a synthesis technique for strictly reactive circuits of inductors and capacitors. Cauer generalized the theorem for other two-element networks of resistor-inductor and resistor-capacitor types (Brune, 1931).

Brune in 1931, under the guidance of Wilhelm Cauer, Norbert Wiener, and Vannevar Bush, provided a proof of the necessary and sufficient conditions for network realizability, known as positive real (PR) (Brune, 1931). Brune further provided a synthesis technique for creating a lumped-element network that matches the behavior prescribed by a PR function. These PR functions

are in the mathematical form of a Padé approximation. An excellent review of circuit theory can be found in Belevitch (1962).

With improvements in radio technology pushing operating frequencies higher and higher, the quasistatic approximations for lumped-element impedances became a limitation. Radar development during the Second World War motivated much of the research, with the creation of scattering parameters to characterize the behavior of microwave waveguides and filters. These scattering parameters incorporated the characteristic impedance of interconnected media, quantifying the reflections and transmissions of incident wave (Montgomery, Dicke, & Purcell, 1948).

1.4 Organization of This Thesis

Several topics related to impedance, its mathematical properties, and some transformations, will be covered in the upcoming chapters.

Chapter 2 reviews some of the basics of impedance as a quasistatic approximation to Maxwell's equations and within the context of network analysis. It also goes over the pole/zero properties of two-type lumped-element networks.

Chapter 3 revisits the results of Brune's positive real (PR) conditions for lumped-element network realization. It also expresses the entire set of Brune impedances in the time domain, concluding with the limited nature of Brune's rational function impedances.

Chapter 4 explores the input impedance to transmission lines, mainly with a focus on uniform, semi-infinite lines. The time- and frequency-domain properties of these lines are given, as well as an explanation into the effects of wave propagation on the mathematical structure of time-domain impedance – the c-finite class.

Chapter 5 introduces the discrete-time impedance and discusses how the bilinear transformation may be used to convert all rational function impedances into a c-finite form. It also discusses transmission line stubs that approximate ideal capacitors and inductors, as well as gives physical intuition into the nature of frequency warping.

Chapter 6 brings together the c-finite and c-infinite classes, comparing and contrasting them, and discussing how they can approximate each other.

Chapter 7 discusses a special Möbius transformation on an impedance. It offers a reformulation of PR in this Möbius-transformed impedance domain, which has an arguably more intuitive mathematical description. A PR testing procedure is given to determine if a rational function describes a PR impedance.

Chapter 8 discusses a special case of the Möbius impedance, called the *reflectance*. The reflectance is a property of c-finite impedances which offers an alternative formulation of Ohm's law in the time domain and a physical interpretation as outbound and inbound waves at a boundary.

Chapter 9 gives conclusions to this thesis.

1.5 Motivation

The underlying motivation for this thesis arises from modeling the cochlea which is a nonlinear, time-varying, active system, often approximated using passive, linear, time-invariant systems. The nature of these approximations as a transmission line, as well as basilar membrane partition impedance, called into question the physical and mathematical properties of impedance itself.

CHAPTER 2

NETWORK ANALYSIS AND LUMPED ELEMENTS

Network analysis describes the mathematical tools and physical assumptions for modeling simple electromagnetic phenomena. The physics for network analysis derives from Maxwell's equations, but makes an assumption that the speed of wave propagation is infinite (or equivalently the geometry of the device approaches zero size, i.e. is small relative to the wavelength). This quasistatic assumption greatly simplifies the mathematical description of the electromagnetic behavior of a circuit. Typically, a circuit is considered to be a set of multiterminal lumped elements connected together by nodes (Valkenburg, 1955). The voltage along a particular node is usually considered to be the same everywhere, consistent with the infinite wave-speed assumption. Kirchhoff's current and voltage laws help formulate the relationship between the voltage and current of all these nodes by solving a set of simultaneous equations. This formulation explicitly assumes that all parts of the ciruit interact simultaneously. A formal technique, known as modified nodal analysis, expresses the model equations for a circuit and is used in SPICE, a popular electrical circuit simulation computer program (Pillage, Rohrer, & Visweswariah, 1994).

While network analysis considers a broad range of electrical devices, such as diodes, transistors, and transformers, only the basic linear lumped-element impedances will be explored. There are three basic lumped impedances: the inductor, capacitor, and resistor. The inductor and capacitor are lossless devices, whereas the resistor is a purely lossy device. The derivations from Maxwell's equation for each of these components all share a common assumption that wave propagation speed is infinite, which is compatible with the assumption of network analysis.

2.1 Quasistatic Approximations

There are three basic spatial inputs to Maxwell's equations: permeability μ, permittivity ϵ, and conductance σ. The speed of wave propagation in vacuo involves the spatial permeability and permittivity and is given as:

$$c = \frac{1}{\sqrt{\mu_0 \epsilon_0}} \tag{2.1}$$

which approximately equals $3 \cdot 10^8$ meters per second. Wave propagation is a fundamental phenomena of electrical systems, although it can be approximated away in a model.

The quasistatic approximations "neglect certain terms in one or both of the Maxwell's curl equations" (Rao, 2004). These approximations are used in developing the physics of the ideal lumped-element circuit components: resistors, capacitors, and inductors.

The ideal inductor stores and delivers energy exclusively from its magnetic field. The basic assumption for the inductor is that magnetic permeability is present ($\mu > 0$), but spatial permittivity and conductance (loss) are zero ($\epsilon = \sigma = 0$). With this assumption, the time-varying magnetic field inside the inductor no longer causes time-varying electric fields to arise. The internal physical assumptions for the inductor is that of a purely magnetic system with infinite wave speed, since $\epsilon = 0$.

The ideal capacitor stores and delivers energy exclusively from its electric field. Its basic assumption is that permittivity is present ($\epsilon > 0$), but its other parameters are zero ($\mu = \sigma = 0$). The time-varying electric fields inside the capacitor no longer cause time-varying magnetic fields. The internal physical assumptions for the capacitor is that of a purely electric system with infinite wave speed, since $\mu = 0$.

The ideal resistor dissipates energy. The assumption here is that the medium is purely conductance ($\sigma > 0$) but both its permeability and permittivity are zero ($\mu = \epsilon = 0$). The internal assumptions for the resistor is that of a purely lossy system with infinite wave speed, since $\mu = \epsilon = 0$.

The internal assumptions for the inductor, capacitor, and resistor are incompatible, but each leads to a condition of infinite wave speed and hence simultaneity. A summary of these assumptions can be found in Table 2.1. These are all quasistatic approximations to Maxwell's equations. The

Table 2.1: Lumped-element assumptions for an inductor, capacitor, and resistor.

Component	Z(s)	μ	ϵ	σ
Inductor	sL	positive	0	0
Capacitor	1/sC	0	positive	0
Resistor	R	0	0	positive

classification as a lumped element arises since each of these components lump together one aspect of the underlying physics (conductance, permittivity, permeability), which is in distinction to a distributed system where these physical aspects are co-located spatially as a density per unit length, area, or volume.

2.2 Pole and Zero Locations

The input impedance across two terminals of a lumped-element network may be expressed as a rational function. The precise properties of this function will be discussed later in Chapter 3. The locations of these poles and zeros are known for two-type networks, meaning networks composed of either inductors and capacitors (LC), resistors and capacitors (RC), or resistors and inductors (RL). A general result for the pole/zero locations of a three-type network (RLC) remains unsolved. In Chapter 7 we will address this unsolved problem. The following subsections offer a brief review of the two-type networks.

2.2.1 Foster's Reactance Theorem of LC networks

Ronald Martin Foster proved that a purely reactive network, composed of lumped capacitors and inductors, has its poles and zeros alternating along the $j\omega$ axis, with either a pole or a zero at the origin (Foster, 1924). These poles and zeros must also satisfy conjugate symmetry. As a result, the order of the numerator and denominator polynomials describing this network must differ by one. Foster offered a synthesis procedure for creating a lumped-element network with those prescribed properties. Figure 2.1 shows an example of two possible LC pole/zero patterns.

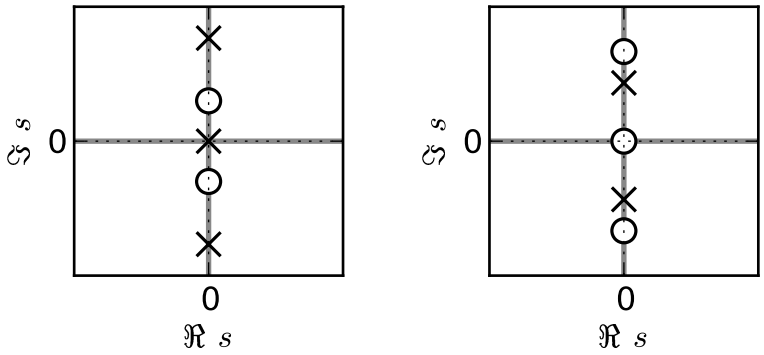

(a) Pole at origin (b) Zero at origin

Figure 2.1: Example placement of poles and zeros for an LC network.

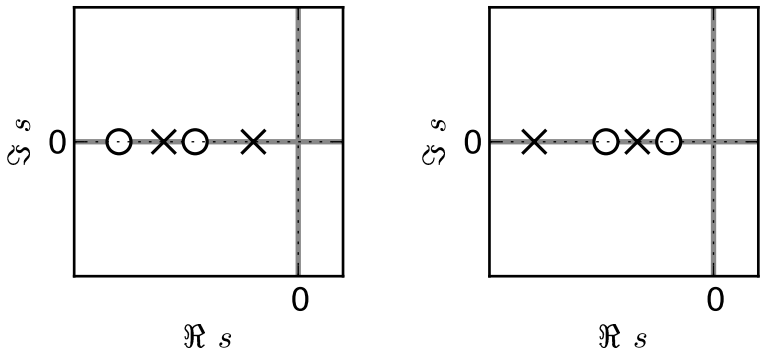

(a) RC network (b) RL network

Figure 2.2: Example placement of poles and zeros for an RC and RL network.

2.2.2 Cauer's Extension to RC and RL networks

Wilhelm Cauer (Brune, 1931) extended Foster's original result for networks composed of resistors and a single type of reactive element (inductor or capacitor). He showed that the poles and zeros alternate along the real σ axis, toward $\sigma = -\infty$. RC networks have a pole closest to the origin; RL networks have a zero closest to the origin. Figure 2.2 shows an example RC and RL pole/zero pattern.

CHAPTER 3

THE BRUNE IMPEDANCE

This chapter will summarize and explain some key points from Brune's original 1931 PhD thesis concerning the nature of passive, rational function impedances. While Brune was not the first to express impedance as a rational function, his findings earned him the category of Brune impedance as a description for rational function impedances.

3.1 Positive Real

Brune proved that positive real (PR) is a necessary and sufficient condition for network realizability. This means that if a given rational function impedance $Z(s)$ satisfies the properties of PR then it is possible to create a lumped-element network with those same properties. Quoting from Brune's abstract (Brune, 1931):

> The necessary and sufficient conditions to be fulfilled by $Z(\lambda)$ are found to be
>
> 1. $Z(\lambda)$ is a rational function (quotient of two polynomials) which is real for real values of λ;
> 2. the real part of $Z(\lambda)$ is positive when the real part of λ is positive; (or $Z(\lambda)$ lies in the right-half Z plane when λ lies in the right-half λ plane).
>
> ...
>
> That it is necessary for $Z(\lambda)$ to be a "positive real" function is readily seen from physical considerations; a contradiction of (1) would mean that a real voltage produces a complex current, which has no physical meaning, while a contradiction of (2) means that the network can under certain conditions generate energy.

Brune used λ instead of s in his original thesis as the complex radian frequency. The remainder of this thesis shall use s instead, where $s = \sigma + j\omega$.

Expressed mathematically, Brune's impedance functions may be written as:

$$Z(s) = \frac{a_0 + a_1 s + a_2 s^2 + ... + a_m s^m}{b_0 + b_1 s + b_2 s^2 + ... + s^n} \tag{3.1}$$

where m and n are the order of the numerator and denominator polynomials, respectively. The highest term in the denominator is normalized to unity instead of being an arbitrary b_n. The first Brune condition can be restated that if $\omega = \Im s = 0$ then $\Im Z(s) = 0$. The second Brune condition can be restated that if $\sigma = \Re s > 0$ then $\Re Z(s) > 0$.

Equation 3.1 is an analytic function in the right-half plane (RHP), since no poles or zeros exist in this region, as well as in most of the left-half plane (LHP) by satisfying Cauchy-Riemann conditions (Greenberg, 1998, p.1140). Singularities exist as poles where the function is not differentiable, hence not analytic. The Cauchy-Riemann conditions are in the form of a Laplace equation which allows the "maximum principle" to apply (Greenberg, 1998, p.1062). This means that the maximum and minimum values of a domain $\mathcal{D}$ satisfying Laplace's equation occur on the boundary of $\mathcal{D}$. Thus the entire RHP has a non-negative real component since the $j\omega$ boundary has a non-negative real component.

These two simple conditions for PR are properties of the real and imaginary parts of the impedance function, but as a result both conditions lead to some interesting emergent properties:

1. Complex poles and zeros have conjugate-symmetric pairs.
2. All poles and zeros are in the left-half plane or on the $j\omega$ boundary (minimum phase).
3. All polynomial coefficients are non-negative.
4. All poles and zeros are simple; no multiplicity.
5. The system is passive: $\Re Z(j\omega) \geq 0$. (Brune, 1931, p.20)
6. The phase angle is bounded between $\pm\frac{\pi}{2}$ when $\Re s \geq 0$. (Brune, 1931, p.20)

7. Order of numerator and denominator polynomials must be within one: $|m - n| \leq 1$.

Complex conjugate pairs for the poles and zeros satisfy the *real* condition, where the time-domain expression must be real-valued in time. Functions with no poles or zeros in the RHP are called "minimum phase" (MP). All impedance functions are MP, which also means that these impedance functions have a causal inverse since no poles (inverted zeros) can exist in the RHP. Inverting an impedance yields a valid admittance function, i.e. $Y(s) = 1/Z(s)$. All passive impedances functions must have a passive admittance.

Brune's original conditions for PR states that when $\sigma > 0$, i.e. the real part of s is strictly positive, then the real part $Z(s)$ is positive. Property 5 arises from a later argument made by Brune that passivity requires the $j\omega$ axis, $\sigma = 0$, be included since values along the $j\omega$ axis correspond to "steady-state" voltages applied to the impedance function $Z(j\omega)$ and these must be passive as well. Brune perhaps should have used "non-negative" instead of "positive" in the definition of positive real, but that would have led to the awkwardly named property of "Non-negative Real".

3.2 Example Circuit

A parallel combination of a resistor, capacitor, and inductor (with all having unity values) has the following impedance formula:

$$Z(s) = \frac{s}{s^2 + s + 1}. \tag{3.2}$$

This impedance has a zero at $s = 0$ and two poles located at $s = \frac{-1}{2} \pm \frac{\sqrt{3}}{2}$. Physically, the values along the $j\omega$ axis are the measurable values of an impedance. Figure 3.1 shows the real and imaginary parts of Eq. 3.2 for a square patch of the complex plane, where $2 \leq \sigma \leq 2$ and $2 \leq \omega \leq 2$.

The real part is non-negative in the entire right-half plane, as shown in Fig. 3.1(a) as a light-blue. The values along the $j\omega$ axis are given in Fig 3.1(b), as a function of ω. The imaginary part is given in Figs. 3.1(c) and 3.1(d).

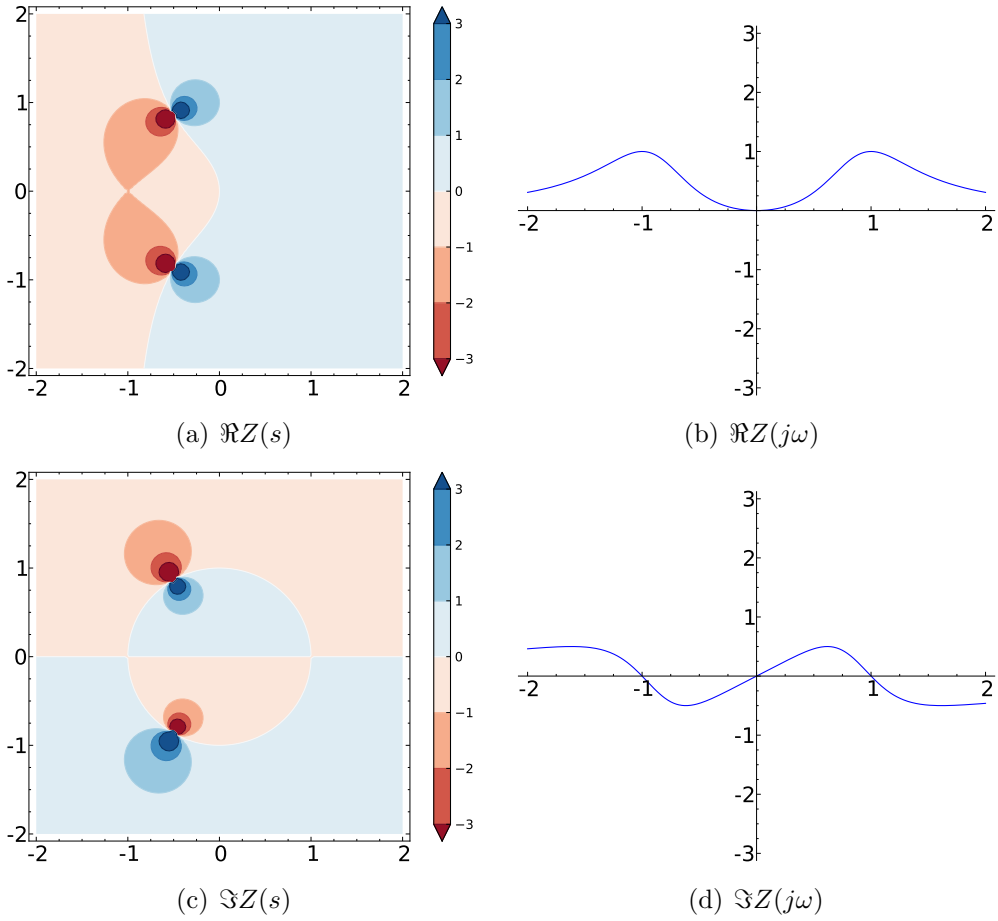

(a) $\Re Z(s)$ (b) $\Re Z(j\omega)$

(c) $\Im Z(s)$ (d) $\Im Z(j\omega)$

Figure 3.1: Real and imaginary parts of Eq. 3.2.

The magnitude and phase are also shown in Fig. 3.2. The magnitude is non-negative, as it should be, with the poles centered in the dark blue circles in Fig. 3.2(a). The phase shown in Fig. 3.2(c) is in degrees, meaning that the RHP must be bound to $\pm 90°$, as is shown by the light blue and red regions and by Fig. 3.2(d) which shows the phase along the $j\omega$ axis.

3.3 Toward a Time-Domain Expression

Brune's rational function expression for an impedance has an equivalent partial fraction expansion. Equation 3.1 may be expanded in the following form:

$$Z(s) = Es + D + \frac{r_1}{s - p_1} + ... + \frac{r_n}{s - p_n} \tag{3.3}$$

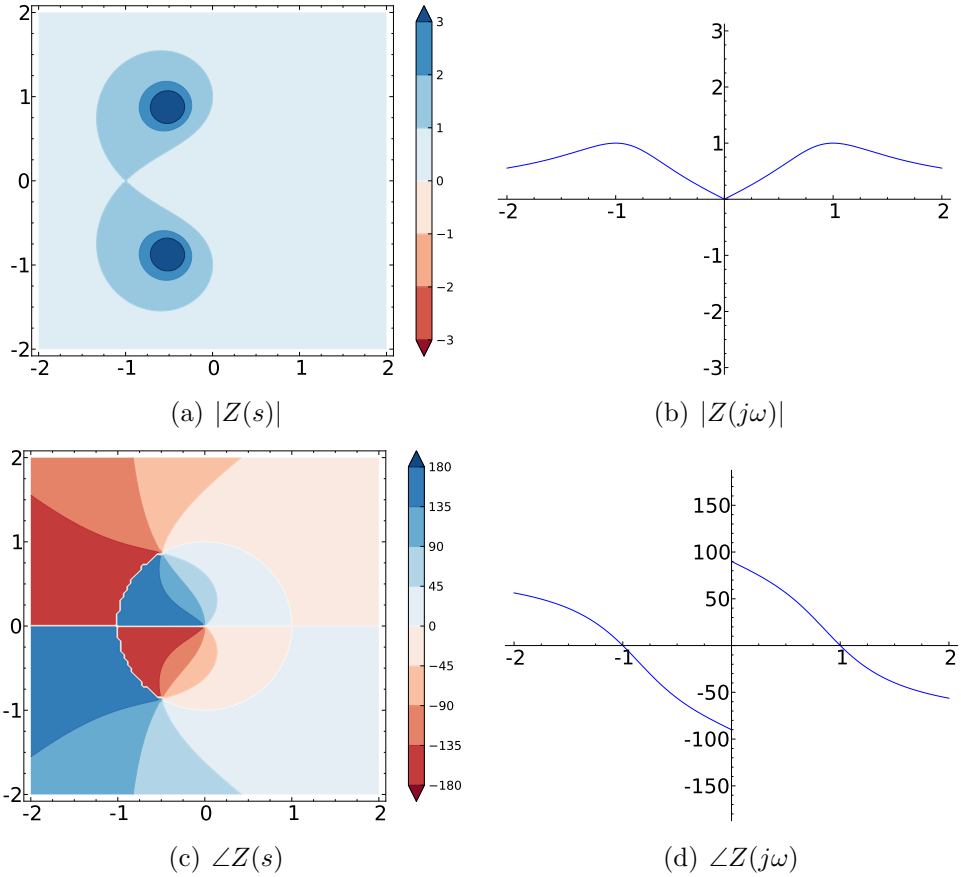

(a) $|Z(s)|$ (b) $|Z(j\omega)|$

(c) $\angle Z(s)$ (d) $\angle Z(j\omega)$

Figure 3.2: Magnitude and phase of Eq. 3.2.

where the poles and residues can be expressed in terms of their real and imaginary components:

$$r_i = x_i + jy_i \tag{3.4}$$

$$p_i = \sigma_i + j\omega_i. \tag{3.5}$$

Complex poles and residues all occur as conjugate pairs, which adds some restriction to the form of the partial fractional expansion. Real poles have real residues. Only a single pole may exist at the origin, which may be considered a special case of the real poles.

The partial fraction expansion for Eq. 3.1 may be more precisely expressed as:

$$Z(s) = \overbrace{Es + D + \frac{r_0}{s}}^{\text{simple terms}} + \overbrace{\sum_k \left(\frac{x_k}{s - \sigma_k} \right)}^{\text{real poles}} + \overbrace{\sum_i \left(\frac{x_i + jy_i}{s - (\sigma_i + j\omega_i)} + \frac{x_i - jy_i}{s - (\sigma_i - j\omega_i)} \right)}^{\text{conjugate poles}}. \tag{3.6}$$

The first three terms compose the simple terms. The lead term Es occurs when the numerator polynomial order is one greater than the denominator ($m = n + 1$). The D term represents frequency-independent behavior of the circuit due to losses in the circuit; however, it is not necessarily a series resistance term. The r_0/s term captures the behavior when a simple pole exists at the origin. For the simplest circuit, these three terms model the behavior of a circuit composed of an inductor, resistor, and capacitor in series. For more complex circuits, these terms may have a different circuit topology interpretation. These lead terms have the following inverse Laplace transform:

$$\overbrace{Es + D + \frac{r_0}{s}}^{\text{simple terms}} \overset{\mathcal{L}^{-1}}{\longleftrightarrow} E\delta'(t) + D\delta(t) + r_0 u(t) \tag{3.7}$$

where $\delta(t)$ represents the Dirac delta distribution, $\delta'(t)$ represents the first derivative of the Dirac delta, and $u(t)$ is the Heaviside step function. Within convolution, the Dirac delta is an identity operator, the time-derivative of the Dirac delta is a time-derivative operator, and the Heaviside step function

represents integration.

The real poles, which lie strictly on the negative real sigma axis, represent exponential decay terms in the time domain. With $r_k = x_k$ and $p_k = \sigma_k$, the Laplace transform pair may be expressed as:

$$\overbrace{\frac{r_k}{s - p_k}}^{\text{real pole}} \overset{\mathcal{L}^{-1}}{\longleftrightarrow} x_k e^{\sigma_k t} u(t) \tag{3.8}$$

All the remaining complex residues and poles occur as conjugate pairs. This means that its time-domain expression is real-valued when taking its inverse Laplace transform. The conjugate poles may be expressed as:

$$\overbrace{\frac{x_i + jy_i}{s - (\sigma_i + j\omega_i)} + \frac{x_i - jy_i}{s - (c_i - jd_i)}}^{\text{conjugate poles}} \overset{\mathcal{L}^{-1}}{\longleftrightarrow} 2\left(x_i \cos(\omega_i t) - y_i \sin(\omega_i t)\right) e^{\sigma_i t} u(t) \tag{3.9}$$

along with its inverse Laplace transform.

In total, the time-domain expression of Eq. 3.6 will have the following form:

$$z(t) = \overbrace{E\delta'(t) + D\delta(t) + r_0 u(t)}^{\text{simple terms}} + \underbrace{\sum_k \left[x_k e^{\sigma_k t} u(t)\right]}_{\text{real poles}} + \underbrace{2\sum_i \left[\left(x_i \cos(\omega_i t) - y_i \sin(\omega_i t)\right) e^{\sigma_i t} u(t)\right]}_{\text{conjugate poles}}. \tag{3.10}$$

Equations 3.6 and 3.10 represent the entire set of mathematical formulations of Brune's impedance in the time and frequency domains. Clearly the rational function formulation of an impedance has many limitations since other mathematical functions exist to describe more general impedances. Chapter 4 will explore irrational and trigonometric impedances.

CHAPTER 4

TRANSMISSION LINE IMPEDANCES

The telegrapher's equations (the TEM solutions to Maxwell's equations) describe the electromagnetic behavior of a transmission line in one spatial variable. It has four per-unit spatial parameters: series resistance $R(x)$, series inductance $L(x)$, shunt conductance $G(x)$, and shunt capacitance $C(x)$. The spatial voltage and current are given by two coupled, first-order differential equations:

$$\frac{\partial}{\partial x}V(x,t) = -L(x)\frac{\partial}{\partial t}I(x,t) - R(x)I(x,t) \tag{4.1}$$

$$\frac{\partial}{\partial x}I(x,t) = -C(x)\frac{\partial}{\partial t}V(x,t) - G(x)V(x,t). \tag{4.2}$$

It is important to note that wave propagation requires both $L(x)$ and $C(x)$ to be greater than zero, otherwise the system of differential equations is no longer hyperbolic (wave equation).

In the lossless, homogeneous case where $R = G = 0$, the equations to the wave equation simplify:

$$\frac{\partial}{\partial x}V(x,t) = -L\frac{\partial}{\partial t}I(x,t) \tag{4.3}$$

$$\frac{\partial}{\partial x}I(x,t) = -C\frac{\partial}{\partial t}V(x,t) \tag{4.4}$$

for which the speed of wave propagation becomes $\frac{1}{\sqrt{LC}}$.

Typically, transmission lines are used as two-port devices, meaning that the line connects two electrical networks. For now, the case of a uniform, semi-infinite line will be considered, where the line begins spatially at $x = 0$ and extends toward $x = +\infty$. The telegrapher's equations exactly describes plane waves propagating along a line. Using separation of variables on the wave equation, it is easy to show that these equations also exactly describe cylindrical and spherical wave propagation (Putland, 1993), but these two

cases will not be further pursued here. (Non-uniform lines are considered in Appendix B.) The uniform line has an input impedance described by:

$$Z(s) = \sqrt{\frac{R + sL}{G + sC}} \tag{4.5}$$

and a propagation function described by:

$$\beta(s) = \sqrt{(R + sL)(G + sC)}. \tag{4.6}$$

Together, these parameters describe a wave traveling along a transmission line. The steady-state phasor representation for the total voltage and net current along the line can be expressed in terms of its forward and backward traveling waves as:

$$\overline{V}(x, s) = \overline{V}^{+} e^{-j\beta(s)x} + \overline{V}^{-} e^{j\beta(s)x} \tag{4.7}$$

$$\overline{I}(x, s) = \frac{1}{Z}\left(\overline{V}^{+} e^{-j\beta(s)x} - \overline{V}^{-} e^{j\beta(s)x}\right) \tag{4.8}$$

where $\overline{V}$, $\overline{V}^{+}$, and $\overline{V}^{-}$ are all phasors. The use of the complex frequency variable s instead of $j\omega$ allows for an analysis in the complex plane instead of the ω axis. This is a more general re-expression of the equations provided in Rao (2004). Otherwise ω would need to become complex, essentially mimicking s anyway.

Several interesting cases emerge from this simple equation when considering both its time and frequency domain properties. Perhaps the most stunning results are the myriad of ways to realize a simple resistor, as discussed in Section 4.5.

4.1 Time-Domain Properties of C-Finite Impedance

All c-finite impedances support wave propagation at the input terminals. By the initial singularity theorem (see Appendix A.1), a uniform transmission line has an initial delta function. Taking the limit as the real part of s approaches positive infinity in Eq. 4.5 gives:

$$\lim_{\Re s \to +\infty} \sqrt{\frac{R + sL}{G + sC}} = \sqrt{\frac{L}{C}} \tag{4.9}$$

Therefore, the time-domain expression of a transmission line input impedance must contain an initial Dirac delta function. This initial response depends only upon the per-unit spatial parameters for inductance and capacitance. *The losses do not affect the response instantly at time* $t = 0$. Also, since the wave propagation speed is finite, the transmission line structure beyond the input at $x = 0$ cannot affect the instantaneous response at the input for $t = 0$. Thus, the spatial parameters could become spatial-varying beyond $x = 0$, meaning this result, of an initial delta function, generalizes to the non-uniform line. A second example of this point is given in Section 4.6, using a uniform line of arbitrary, finite length terminated in an arbitrary impedance.

Thus, as stated by Eq. 1.1 and again here, all c-finite impedances have the following time-domain formulation:

$$z(t) = R_0\delta(t) + z_{res}(t)u(t)$$

where R_0 represents the surge impedance of the c-finite impedance and $z_{res}(t)$ captures the effects of reactive waves (stored energy) returning to the input and being reflected back into the transmission line.

4.1.1 Example c-finite impedance

Consider a finite-length, uniform, lossless transmission line, terminated in an open circuit. This open-circuit condition makes its far-end reflection coefficient equal unity. Also, add the constraint that the round-trip travel time for a wave equals unity time. This requires that the length $\mathfrak{L}$ and the speed c be related by $\frac{2\mathfrak{L}}{c} = 1$. The time-domain response may then be expressed as:

$$z(t) = \overbrace{\delta(t)}^{\text{surge}} + \overbrace{2\delta(t-1) + 2\delta(t-2) + 2\delta(t-3) + ...}^{\text{residual}} \tag{4.10}$$

where the train of twice-unity delta functions continues forever. The input boundary reflection coefficient is also unity by the nature of the line being driven by an ideal current source providing an impulse. The time-domain expression of this impedance is of the form described in Eq. 1.1.

The frequency-domain expression for this line is given as:

$$Z(s) = -j \cot\left(s/(2j)\right) \tag{4.11}$$

and can be derived directly from taking the Laplace transform of Eq. 4.10 (in the limit approaching the region of convergence). This is a trigonometric impedance function which behaves differently from the irrational functions given earlier in Eq. 4.5. Applying the initial singularity theorem to Eq. 4.11 gives:

$$\lim_{\Re s \to +\infty} -j \cot\left(s/(2j)\right) = 1 \tag{4.12}$$

which is the surge impedance of the line (see Eq. 4.10).

4.2 Uniform Transmission Line Parameters

The four parameters for the uniform transmission line may be chosen to either allow or disallow wave propagation. All possible combinations will be explored, with comments on their time-domain properties. Many of the inverse Laplace transforms used here can be found in Table A.1.

4.3 Line as a C-Finite Impedance

When both L and C are positive, then the input impedance in Eq. 4.5 has wave propagation. The impedance may be re-expressed as:

$$Z(s) = \sqrt{\frac{L}{C}} \sqrt{\frac{\frac{R}{L} + s}{\frac{G}{C} + s}} \tag{4.13}$$

A closed-form inverse Laplace transform exists for this equation (Table A.1):

$$z(t) = \overbrace{\sqrt{\frac{L}{C}}\delta(t)}^{\text{surge}} + \underbrace{\frac{1}{2}\sqrt{\frac{L}{C}}\left(\alpha - \beta\right) e^{\frac{-(\alpha+\beta)t}{2}} \left[I_1\left(\frac{1}{2}(\alpha-\beta)t\right) + I_0\left(\frac{1}{2}(\alpha-\beta)t\right)\right] u(t)}_{\text{residual}} \tag{4.14}$$

where $\alpha = \frac{R}{L}$ and $\beta = \frac{G}{C}$. The I_1 and I_0 functions are modified Bessel functions.

When $\frac{R}{L} = \frac{G}{C}$, the condition for distortionless transmission is met, as given by Heaviside (Heaviside, 1950, 1:367). In this case, the residual portion of the input impedance goes to zero, which is consistent with the physical result of distortionless transmission, as these distortions caused by dispersion create a residual response after the initial pulse.

4.4 Line as a C-Infinite Impedance

Setting either $L = 0$ or $C = 0$ disallows wave propagation in the line model, thus making it fall into the c-infinite class. The system becomes a diffusion line, which is useful when describing thermal systems at low frequencies. None of these c-infinite line impedances have a $\delta(t)$ surge impedance term in their time-domain expression.

4.4.1 The semi-capacitor

When the per-unit-length inductance goes to zero, hence $L = 0$, the input impedance can be expressed as:

$$Z(s) = \sqrt{\frac{R}{G + sC}} = \sqrt{\frac{R}{C}}\sqrt{\frac{1}{\frac{G}{C} + s}} \tag{4.15}$$

which has the following time-domain representation:

$$z(t) = \sqrt{\frac{R}{C}}\frac{1}{\sqrt{\pi t}}e^{-\alpha t}\,u(t) \tag{4.16}$$

with $\alpha = \frac{G}{C}$. Notice that as $t \to 0^+$ the time-domain expression approaches infinity. Since the impedance is causal, the discontinuity at $t = 0$ must be considered when taking this limit. This singularity is not the same as the Dirac delta singularity. When $\alpha = 0$, this system describes a semi-capacitor, with the form $\frac{1}{\sqrt{s}}$, used to describe heat diffusion.

4.4.2 The semi-inductor

When $C = 0$, the input impedance can be expressed as:

$$Z(s) = \sqrt{\frac{R + sL}{G}} = \sqrt{\frac{L}{G}}\sqrt{\frac{\frac{R}{L} + s}{1}} \tag{4.17}$$

which has the following time-domain representation:

$$z(t) = \frac{1}{2}\sqrt{\frac{L}{G}}\frac{-1}{\sqrt{\pi t^3}}e^{-\beta t}\,u(t) \tag{4.18}$$

with $\beta = \frac{R}{L}$. When $\beta = 0$, the system describes a semi-inductor with the form $\sqrt{s}$, used to describe magnetic field diffusion into an iron core with eddy currents (Vanderkooy, 1989). This impedance becomes useful when modeling electromagnetic loudspeakers.

Like the semi-capacitor, the semi-inductor time-domain expression approaches infinity as $t \to 0^+$

4.5 Pure Loss (Resistor)

The line may be used to model a pure loss impedance, i.e. a resistor, either as c-finite or c-infinite. A resistor has the following frequency- and time-domain expressions:

$$Z(s) = R_0 \tag{4.19}$$

$$z(t) = R_0\delta(t) \tag{4.20}$$

The parameters for the uniform transmission line may be chosen to mimic this input impedance by several ways, as a c-finite or a c-infinite impedance.

The c-finite case requires that both L and C be positive. When $R/L = G/C$, the transmission line has spatial losses, but its time-domain expression is equivalent to a resistor.

$$Z_0(s) = \sqrt{\frac{L}{C}}\sqrt{\frac{\frac{R}{L} + s}{\frac{G}{C} + s}} = \sqrt{\frac{L}{C}} \overset{\mathcal{L}^{-1}}{\Longleftrightarrow} z(t) = \sqrt{\frac{L}{C}}\delta(t) \tag{4.21}$$

A special case of this c-finite form involves setting all losses to zero, i.e.

$R = G = 0$. This creates a lossless transmission line, but its time-domain expression is still equivalent to a resistor.

$$Z_0(s) = \sqrt{\frac{sL}{sC}} = \sqrt{\frac{L}{C}} \overset{\mathcal{L}^{-1}}{\Longleftrightarrow} z(t) = \sqrt{\frac{L}{C}}\delta(t) \tag{4.22}$$

The initial wave entering into the transmission line continues forever toward $x = +\infty$. For all intents and purposes, this energy is lost as it never returns. From this construction it is possible to realize a pure loss resistor by using a *lossless* transmission line. It is at least interesting that different theoretical realizations of a resistor have thus been shown to exist.

Another possible way to achieve a pure loss is to set both $L = C = 0$, which disallows wave propagation. The line describes a c-infinite impedance and is a spatially distributed loss.

$$Z_0(s) = \sqrt{\frac{R}{G}} \overset{\mathcal{L}^{-1}}{\Longleftrightarrow} z(t) = \sqrt{\frac{R}{G}}\delta(t) \tag{4.23}$$

From these simple configurations, a system with the equivalent input impedance of a resistor can be realized. This pure loss can be realized as a semi-infinite line with wave propagation (c-finite) or a purely lossy line with no distributive reactance (c-infinite).

4.6 Loaded Transmission Lines

A second application of the transmission line is to connect two separate systems (requiring the line to be of finite length). The two-port representation as a T-matrix is:

$$T = \begin{bmatrix} \cosh(\beta\mathfrak{L}) & Z_0 \sinh(\beta\mathfrak{L}) \\ \frac{1}{Z_0}\sinh(\beta\mathfrak{L}) & \cosh(\beta\mathfrak{L}) \end{bmatrix} \tag{4.24}$$

where β is propagation function from Eq. 4.6, Z_0 is the characteristic impedance of the line from Eq. 4.5, and $\mathfrak{L}$ is the length of the line.

If the line is terminated with a one-port impedance Z_L, then the input

impedance to the total system becomes:

$$Z_{in} = Z_0 \frac{Z_L \cosh(\beta\mathfrak{L}) + Z_0 \sinh(\beta\mathfrak{L})}{Z_L \sinh(\beta\mathfrak{L}) + Z_0 \cosh(\beta\mathfrak{L})} \tag{4.25}$$

In the limit as $\mathfrak{L} \to 0$, the input impedance becomes simply Z_L since the transmission line no longer separates the input from the Z_L network.

By the initial singularity theorem, the limit as $\Re(\beta\mathfrak{L}) \to +\infty$ gives $\sqrt{L/C}$, which is the surge impedance of the line network itself. This may be considered an alternative approach to the result of Section 4.1.

4.7 Branch Cuts and Positive Real

All the irrational impedances described in this chapter have branch cuts. The square root is a "multi-valued" function, i.e. it has two possible solutions which square to the original value. The branch cut is a way to "take multi-valued functions and render them single-valued." (Greenberg, 1998, p.1131). The proper solution to this problem is to choose the branch such that the value satisfies PR.

As an example, take the case of the unit semi-inductor $\sqrt{s}$. This function can be expressed in polar form:

$$\sqrt{s} = (re^{j(\theta_0+2k\pi)})^{1/2} = r^{1/2}e^{\theta_0/2}e^{k\pi} \quad k \in [0,1] \tag{4.26}$$

where $r = |s|$, the magnitude (modulus) of s, and θ_0 is the angle (argument) of s (Greenberg, 1998, p.1128). The value of k permits the two solutions for the square root, which amounts to adding more phase to the value. The $\pm$ on the output of a square root amounts to π phase difference.

PR requires that this phase be bound to $\pm\frac{\pi}{2}$ when $\Re s \geq 0$. When $k = 0$, then the phase for Eq. 4.26 is bound to $\pm\frac{\pi}{4}$ which satisfies PR. The other branch for $k = 1$ causes the value to violate PR since it adds π phase to the complex value, essentially multiplying the $k = 0$ value by -1.

CHAPTER 5

THE BILINEAR TRANSFORM AND DISCRETE-TIME IMPEDANCE

The bilinear transform is a special type of Möbius transform commonly used for converting analog transfer functions in the s variable to digital transfer function in the z variable. It is a variable substitution given by:

$$s = \frac{2}{T}\frac{1 - \mathrm{z}^{-1}}{1 + \mathrm{z}^{-1}} \tag{5.1}$$

where T is the sampling period. It may be thought of as a first-order approximation of a delay by one sample period T, that is $\mathrm{z}^{-1} = e^{-sT}$ when comparing the z-transform and Laplace transform:

$$\overbrace{X(\mathrm{z}) = \sum_{n=0}^{\infty} x[n]\,\mathrm{z}^{-n}}^{\text{z-transform}} \qquad \overbrace{X(s) = \int_{0^-}^{\infty} x(t)\,e^{-st}dt}^{\text{Laplace transform}}. \tag{5.2}$$

Discrete-time systems have a continuous time interpretation as a sequence of periodic weighted Dirac delta functions, convolved with a suitable low-pass, anti-aliasing filter. Such discrete-time systems are viewed as essentially band-limited, but in fact are periodic in frequency.

5.1 Discrete-Time Impedance

Consider, next, the discrete-time representation without any anti-aliasing filter. The sequence of periodic delta functions would represent the impulse response for a chain of "discretized" two-port transmission lines, composed of uniform, lossless segments with different characteristic impedances. Figure 5.1 shows such a network.

The voltage response to a current impulse reveals a discrete-time input impedance. This time-domain input impedance is of the form of a c-finite

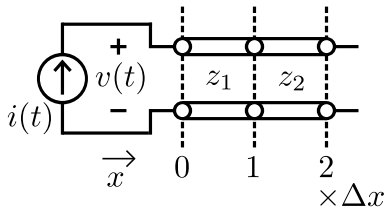

Figure 5.1: A short transmission line stub network.

impedance, as described by Eq. 1.1.

In other words, a bilinear transformation of a rational PR impedance function gives a c-finite impedance. Alternatively, by using known network synthesis techniques, a lumped element network may be transformed to an equivalent wave digital filter (WDF) network (Fettweis, 1986). A WDF network necessarily describes a c-finite impedance.

5.2 Stub Approximations

The ideal capacitor and inductor impedances are quasistatic approximations to a transmission line. This interpretation requires the wave-speed to approach infinity, which is the same as letting the physical geometry of the system approach zero size. These are equivalent interpretations of the network theory concept.

The lossless uniform transmission line having an open-circuit termination describes the behavior of a capacitor at low frequencies. Figure 5.2(a) shows the impedance of an ideal capacitor and the stub-equivalent. Similarly, a short-circuit termination describes the behavior of an inductor, as shown in Fig. 5.2(b). These are simple WDF networks.

Consider for a moment that each capacitor and inductor in a Brune impedance network gets replaced by its transmission line stub equivalent, where each line has the same length and wave-speed. The interconnects between these circuit components, however, will still be instantaneous, just as it is in classical network theory. This modified network is a first step toward including wave propagation in the original c-infinite network of lumped capacitors and inductors.

For a given current impulse, a traveling wave enters each of these transmission line stubs and reflects off the termination. Since all these stubs

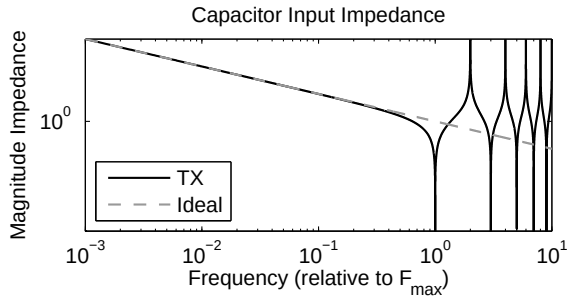

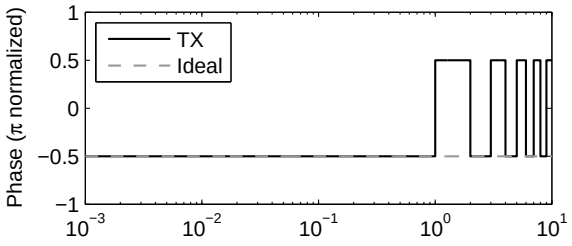

(a) Capacitor input impedance

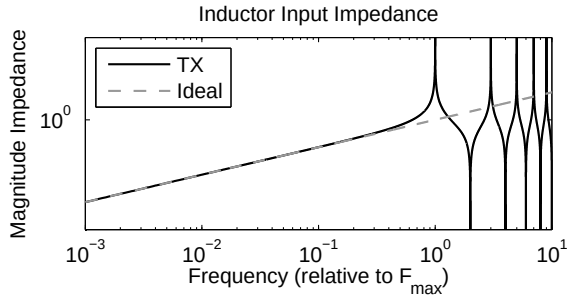

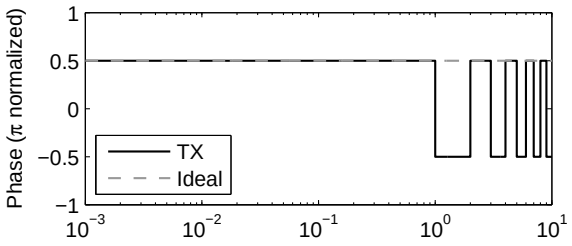

(b) Inductor input impedance

Figure 5.2: TX line stub and ideal component impedances.

are the same length, the response voltage will be periodic, separated by $2\mathfrak{L}/c$, the round-trip travel time along a length $\mathfrak{L}$ line with wave speed c.

This new network is the mathematical equivalent of taking the Brune rational polynomial and performing a bilinear transformation from Eq. 5.1, where the sampling period equals the round-trip wave-travel time of a short stub of transmission line, i.e. $T = 2\mathfrak{L}/c$.

5.3 Input Impedance to Elements

In the derivation of a discrete-time domain representation of a capacitor and an inductor, a transmission line emerged from the mathematics as a consequence of the bilinear transform. Capacitors and inductors originate from quasistatic approximations of transmission lines with different terminating boundary conditions. For the sake of completeness, a resistor can be thought of as a TX line stub with a matched termination.

A TX line model of a capacitor has an open-circuit termination. Let T represent the round-trip delay of a wave propagating along the TX line. The input impedance a transmission line model of a capacitor can be expressed as (Johns & O'Brien, 1980):

$$Z_C(s) = \frac{T}{2C}\coth(s\frac{T}{2}) \tag{5.3}$$

$$\approx \frac{1}{sC} + \frac{sT^2}{12C} - \frac{s^3T^4}{720C} + \cdots \tag{5.4}$$

The first term of its Taylor series expansion gives the quasistatic impedance of $Z_C = \frac{1}{sC}$. The time-domain expression of Eq. 5.3 can be expressed as:

$$z_C(t) = \delta(t) + 2\sum_{n=1}^{\infty}\delta(t - nT) \tag{5.5}$$

and is identical to the system described earlier in Eq. 4.10 when $T = 1$.

The inductor transmission line model with a short circuit termination has

an input impedance of:

$$Z_L = \frac{2L}{T}\tanh(s\frac{T}{2}) \tag{5.6}$$

$$\approx sL - \frac{s^3LT^2}{12} + \frac{s^5LT^4}{120} + \cdots \tag{5.7}$$

Its first Taylor series expansion term gives the quasistatic impedance of $Z_L = sL$. The time-domain expression of Eq. 5.6 is similar to that of the capacitor, but the short-circuit termination has a negative reflection coefficient. This shorted termination causes the delayed Dirac delta functions to alternate in sign, given as:

$$z_L(t) = \delta(t) + 2\sum_{n=1}^{\infty}(-1)^n\delta(t - nT) \tag{5.8}$$

The frequency for input impedance of ideal quasistatic components and their transmission-line models in Fig. 5.2 extends beyond F_{max}. Frequencies beyond F_{max} cannot exist in the discrete-time domain because of the Nyquist criterion. These higher frequencies are plotted merely to show the alternating pole and zero input impedance pattern. These higher frequencies in the transmission line model behave identically to frequency aliasing in the discrete-time model.

At $F_{max} = 1/(2T)$, the input impedance to each component matches the impedance of the quasistatic component at $F = \infty$. Let ω_a be the frequency for the analog quasistatic capacitor, and let ω_d be the digital frequency input to a transmission line model of a capacitor. Setting the impedance for the quasistatic model Z_{C_a} equal to digital transmission line model Z_{C_d} will give the relationship between analog and digital frequency:

$$Z_{C_a} = Z_{C_d} \tag{5.9}$$

$$\frac{1}{j\omega_a C} = \frac{T}{2C}\coth(j\omega_d\frac{T}{2}) \tag{5.10}$$

$$j\omega_a = \frac{2}{T}\tanh(j\omega_d\frac{T}{2}) \tag{5.11}$$

$$\omega_a = \frac{2}{T}\tan(\omega_d\frac{T}{2}) \tag{5.12}$$

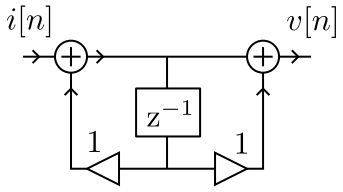

Figure 5.3: Signal flow diagram for implementing Ohm's law for a discrete-time capacitor $z_C(t)$.

5.3.1 Frequency Warping

There is a nonlinear frequency mapping between the digital frequency input impedance of a component as compared to analog input impedance of the ideal quasistatic component. Although frequency-warping due to the bilinear transform has been known, this interpretation gives a physically motivated reason for it; the bilinear transform replaces quasistatic components with transmission line stubs. Equation 5.12 is simply the model for frequency warping. *What this shows is that discrete-time impedance is present in digital signal processing, but unrecognized for what it is.*

5.4 Discrete Realization

Applying the bilinear transform to a rational function impedance in s gives a rational function in z^{-1} which has an implementation using unit delay elements and an interpretation as a discrete-time impedance. These impedances become filter kernels within the context of Ohm's law, where the input signal $i[n]$ is the current and the output signal is the voltage $v[n]$.

5.4.1 Capacitor

The discrete-time version of Eq. 5.5 indexes uses integer n, where $z_C(nT) = z_C[n]$. The $z_C[n]$ implements Ohm's law as an IIR filter kernel as shown in Fig. 5.3.

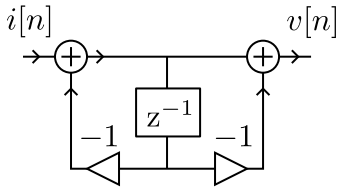

Figure 5.4: Signal flow diagram for implementing Ohm's law for a discrete-time inductor $z_L(t)$.

5.4.2 Inductor

The discrete-time version of Eq. 5.8 indexes uses integer n, where $z_L(nT) = z_L[n]$. The $z_L[n]$ implements Ohm's law as an IIR filter kernel as shown in Fig. 5.4. Note that this figure is the direct form II realization of Fig. 5.1 if both stubs have the same characteristic impedance and $T = 2$.

CHAPTER 6

THE C-INFINITE AND C-FINITE IMPEDANCE CLASSES

The c-finite and c-infinite classes describe the physical wave-speed assumptions in an impedance model. Lumped-element networks are c-infinite, as discussed in Chapter 2. Transmission lines can be either c-finite or c-infinite, as discussed in Chapter 4. This chapter will discuss the similarities and differences of these two classes.

6.1 The C-Finite Class

The c-finite impedance class describes systems that are non-simultaneous due to the finite delay of waves propagating from one part to another. We assume each member of this class has the time-domain formulation given in Eq. 1.1. The surge impedance R_0 itself is of the form of a resistance as described in Section 4.5, but in reality it represents the initial outbound wave into the impedance structure. The energy contained in this wave may fully return to the input, meaning that the impedance network is purely *reactive*. A short stub of transmission line described in Section 4.1.1 demonstrates this point.

The required initial Dirac delta form also holds true for a time-domain admittance expression:

$$y(t) = \frac{1}{R_0}\delta(t) + y_{res}(t)u(t) \tag{6.1}$$

which follows from the same derivation for Eq. 1.1.

6.1.1 Realization of C-Finite

Sondhi and Gopinath (1971) showed that any time-domain c-finite impedance may be expressed as an equivalent acoustic area function. By assuming

uniform wave-speed throughout the system, the spatial volume up to position $x = a$ may be solved using their Eq. 10:

$$V(a) = \int_0^a f(a,t)dt \tag{6.2}$$

where $f(a,t)$ is the solution to the Fredholm integral equation given by their Eq. 8:

$$f(a,t) + \frac{1}{2}\int_{-a}^{a} h(|t-\tau|)f(a,\tau)d\tau = 1, \quad |t| \leq a \tag{6.3}$$

where $h(t) = \frac{1}{R_0} z_{res}(t)$ of Eq. 1.1. This volume is equivalent to the total capacity of the transmission line in an electrical system. Caflisch (1981) provided the discrete version of this result for an electrical line, where the spatial distribution of capacitances are not continuous but composed of segments of uniform, equi-length line. Figure 5.1 shows a trivial example for two segments.

The Sondhi-Gopinath theory assumes a lossless transmission line, meaning if $z(t)$ describes a lossy c-finite impedance, then the solution extends outward indefinitely. This indefinite line extension is related to how a semi-infinite transmission line may be used to model a pure loss, as shown in Section 4.5. In fact, $f(a,t) = 1$ is the solution for a pure loss, which describes the semi-infinite line exactly.

6.2 Rational Function Impedances as C-Finite

The lumped-element Brune impedance (Chapter 2) takes the form of a rational function. When the numerator and denominator polynomials are of the same order ($m = n$) the time-domain expression will share the form of a c-finite impedance. This "ambiguity" of the wave-speed assumption may be useful for modeling wave systems with rational functions, but only for lossy wave systems, as will be shown. While Brune's PR proves that this rational function has a lumped-element representation, it has also a valid realization as a wave propagation impedance in a non-uniform transmission line (Sondhi & Gopinath, 1971). The ability to realize an equi-order rational impedance either as a lumped-element network or as a spatially-varying, semi-infinite line represents a fundamental *duality* for this subset of rational impedance

representations. Succinctly, a lumped or distributed network may be used to realize this network *exactly*, but under different physical assumptions (c-infinite or c-finite).

Lossless rational functions, according to Foster's reactance theorem, require that the order of the numerator and denominator polynomials differ by one ($|m - n| = 1$) so that either a pole or a zero exists at $s = \infty$. With this constraint, a lossless rational function impedance cannot be in the form of a c-finite impedance, as the initial singularity may be a $\delta'(t)$ for a zero at the origin, or a unit step $u(t)$ for a pole at the origin. Therefore, *if the order of the numerator and denominator polynomials are of the same order, the network must contain losses.*

The initial Dirac delta in the time-domain expression of a rational function c-finite impedance is always a loss term, as this energy never returns to the input. Such requirements make using rational functions an attractive approximation, or sometimes evan an exact representation, for modeling a radiation impedance, as radiation impedances tend to be lossy. (A lossless radiation impedance means that the radiator doesn't actually radiate energy!)

6.2.1 Example Acoustic Radiation Impedance and Admittance

Electro-acoustic analogies exist, where the behavior of an acoustic system may be expressed in terms of electrical parameters due to the underlying mathematics of acoustics and electrics sharing a common form. One simple case of using this electro-acoustic analogy is for a spherical radiator. The radiation impedance of this system is modeled exactly as a resistor in parallel with an inductor. The resistor is the characteristic impedance of the medium, while the inductor is a function of the sphere's surface area.

Kinsler, Frey, Coppens, and Sanders (2000, p.187) describe the radiation impedance of a spherical radiator as:

$$Z_r = \rho_0 c S \cos(\theta_a) e^{j\theta_a} \tag{6.4}$$

where ρ_0 is the density of the medium, c is the wave speed, $S = 4\pi a^2$ is the surface area of the sphere, a is the sphere's radius, $\cot(\theta_a) = ka$, and

$k = \frac{\omega}{c}$ as the wave number. (Could this expression be any more obtuse?) The derivation of this result can be found in Appendix B.1.

Through some algebraic manipulation and Euler's identity, the expression for this radiation impedance may be written simply as:

$$Z_r(s) = \frac{1}{\frac{1}{R} + \frac{1}{sL}} = \frac{sLR}{sL + R} \tag{6.5}$$

where $R = \rho_0 cS$ and $L = \rho_0 Sa$. The time-domain expression for this radiation impedance becomes:

$$z_r(t) = R\delta(t) - \frac{R^2}{L} e^{-\frac{R}{L}t} \tag{6.6}$$

which is of the form of a c-finite impedance (as expected). The surge impedance is R, which represents the energy lost as the spherical wave spatially approaches infinity.

When expressed as an admittance, the time- and frequency-domain expressions simplify greatly. The admittance is given as:

$$Y_r(s) = \frac{1}{R} + \frac{1}{sL} \tag{6.7}$$

The conductance (real part) is *not* a function of s, whereas the resistance (real part) of $Z_r(s)$ is a function of s (when $s = j\omega$). The given admittance form in Eq. 6.7 does not mix energy loss and energy storage terms, which leads to an interesting consequence for its time-domain expression, given as:

$$y_r(t) = \frac{1}{R}\delta(t) + \frac{1}{L}u(t) \tag{6.8}$$

The surge term is the energy loss, and the reactance term is a simple, undamped step function. The loss and storage terms are separate in the time domain as well. This admittance formulation offers a much simpler expression for the physical system than its equivalent impedance formulation since the resistive component $1/R$ is independent of frequency. This point is entirely lost in Eq. 6.4.

6.3 The C-Infinite class

The c-infinite impedance class describes all other impedances that lack wave propagation. These are simultaneous systems, as all parts of the system interact immediately due to infinite wave speed. The lumped-element systems, as discussed in Chapter 2 are also c-infinite, as well as quasistatic. Other c-infinite impedances, such as the diffusion equation, are used to model heat flow. Yet, these are distributed systems, not lumped.

From a mathematics point of view, the class of second-order partial differential equations falls into three categories: parabolic, hyperbolic, and elliptic (Greenberg, 1998, p.947). These partial differential equations may be used to describe a large set of physics. The parabolic category describes the diffusion equation while the elliptic category describes the Laplace equation. These two categories describe the underlying physical model of c-infinite impedances. The hyperbolic class described wave-propagation, the c-finite impedance class.

The term "quasistatic" makes certain non-physical assumptions about the governing equations by omitting terms or neglecting certain coupling effects (Rao, 2004). Quasistatic approximations to the wave equation create a non-physical c-infinite system, a point seemingly lost in the existing engineering literature. However, if the underlying physics is not in the form of a wave-equation (like the heat equation), then there are no quasistatic approximations to make to arrive at the c-infinite condition. Because impedance concepts exist in other physical domains, such as mechanics, acoustics, and thermodynamics, the term "c-infinite" is used here rather than "quasistatic". When restricted to just the electromagnetic domain, then "quasistatic" and "c-infinite" are identical, because any approximation to Maxwell's equations which omits wave propagation must be a quasistatic approximation.

All c-infinite impedances are part of locally simultaneous networks, requiring solutions to simultaneous systems of equations. If the entire network makes the c-infinite assumption, then the network is globally simultaneous.

6.4 Frequency Domain Manipulation

Working with impedance exclusively in the frequency domain has obscured this fundamental distinction between c-finite and c-infinite impedances. These classes may be combined in a circuit representation by using the c-infinite assumptions of network analysis. As a consequence, the physical assumptions underlying each network have become distorted, which is the likely reason why the distinction between c-finite and c-infinite has not been explicitly made in the literature (to the best of the author's knowledge).

Take, for example, a lossless transmission line and its lumped-element ladder network approximation. At low frequencies, these networks behave nearly identically, but the time-domain expressions of these two networks are very different. A lossless transmission line has a surge impedance while its approximation as a lossless ladder network of inductors and capacitors becomes a spatially simultaneous low-pass filter (input impedance goes to zero (initial shunt capacitance) or infinity (initial series inductance)).

6.4.1 Middle Ear Modeling

The human middle ear is an excellent illustration of these points. The ear canal acts as a transmission line, a c-finite impedance, terminated with the tympanic membrane (TM), modeled as either a c-finite or c-infinite impedance. The ossicle chain linking the TM to the inner ear is usually modeled mechanically as lumped elements, which are c-infinite impedances. Since the inner ear has small, but finite loss, the c-infinite portion may be modeled using an equi-order rational function, which has a dual interpretation as a wave system (see Section 6.2). Together, a more accurate frequency- and time-domain model may be realized by paying close attention to the underlying c-finite and c-infinite assumptions of the model. Such considerations were explicitly made in the time-domain model by Parent and Allen (2007), with reproductions of the ear canal and ossicle chain models shown in Fig. 6.1. The triangles in the signal flow diagram of the ossicle chain represent "frequency-dependent reflectance filters" (Parent & Allen, 2007).

The discretization process used for the ossicle chain lumped elements was identical to the bilinear transformation detailed in Chapter 5, which effectively translates a c-infinite impedance to a c-finite impedance for the

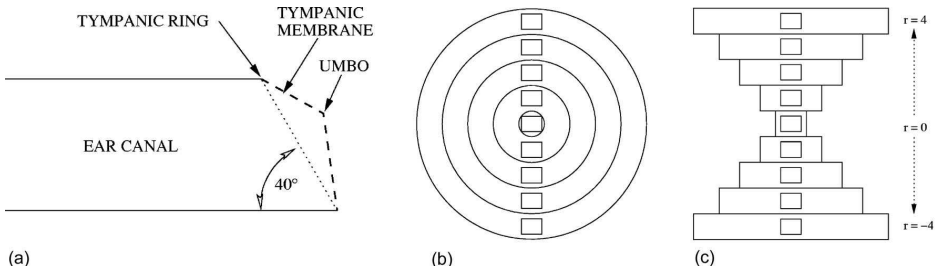

(a) Ear canal model as annuli (c-finite)

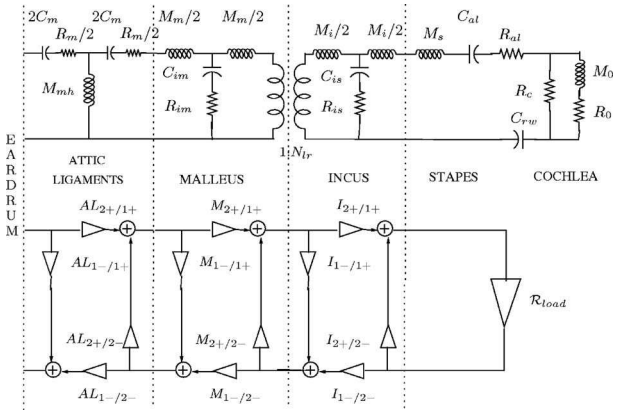

(b) Ossicle chain model as lumped elements (c-infinite) converted to a wave model (c-finite).

Figure 6.1: Reproductions of Figs. 2 and 5 from Parent and Allen (2007).

purposed of discrete-time modeling.

6.5 Interlinking C-Infinite and C-Finite

The c-finite and c-infinite classes may be used to approximate each other by various means. All c-infinite rational functions may be re-expressed using a bilinear transform to give c-finite expressions (see Chapter 5). Equi-order rational impedances have a dual interpretation as both a c-finite and c-infinite network. Taylor series approximations to c-finite transmission line stubs give the c-infinite inductor and capacitor impedances, as shown in Section 5.3. Other mathematical tools exist that may be used to interlink the c-finite and the c-infinite.

6.5.1 Padé Approximations

Padé approximations of a function $Z(s)$ may be expressed as rational functions, whose Taylor series match for the first $m + n + 1$ terms, where m and n are the numerator and denominator polynomial orders, respectively (Press, Teukolsky, Vetterling, & Flannery, 2007, Sec. 5.12). Figure 6.2 shows these relationships for the Padé approximation graphically. As an example, setting $n = 0$ reduces the Padé approximation to just a truncated Taylor series of the original function.

Not all Padé approximations obey PR, despite satisfying $|m - n| \leq 1$. A test for PR is given in Section 7.2. It is important to understand that the entire set of rational impedances are in the form of a Padé approximation, as it suggests the possibility of finding a more accurate expression for modeling the network.

For example, the approach taken in Lin and Kuh (1992) performs a equi-order Padé approximation on the residual part of a *lossy* transmission line impedance, designed to preserve the surge impedance. They accomplish this by taking the approximation for $Z(1/y)$ around $y = 0$, which effectively takes the approximation "around $s = \infty$ because high frequency responses are more important" (Lin & Kuh, 1992). Expressing $Z(1/y)$ as a Padé approximation around $y = 0$ describes the behavior at high frequencies of s. Re-substituing $y = 1/s$ into the equation gives a Padé approximation around $s = \infty$, which

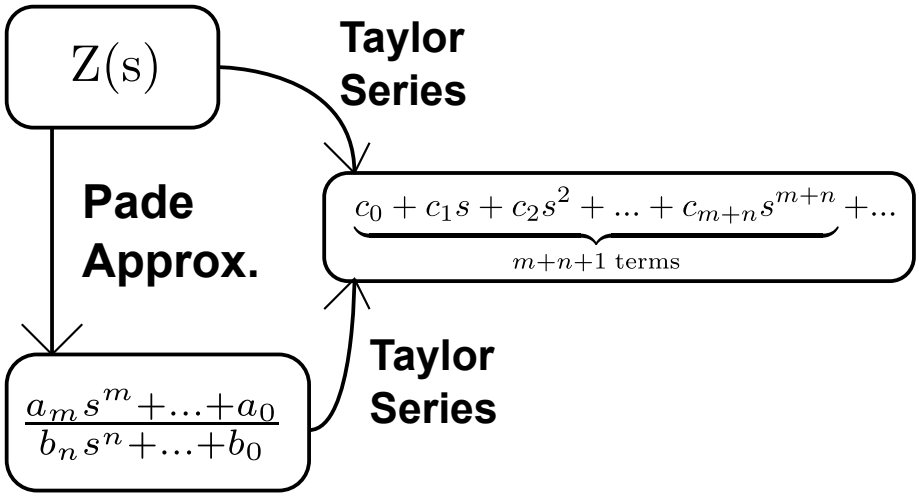

Figure 6.2: A depiction of the Padé approximation and its relation to the Taylor series.

potentially provides a better approximation in the time domain, because it captures transient rather than DC behavior. By the initial singularity theorem, Lin and Kuh's result automatically gives $\sqrt{L/C}$ for the initial time-domain delta function scaling, but physically the initial delta function represents initial resistive losses, not the true surge impedance. Their method does not work on lossless lines (see Section 6.2), a point not acknowledged by Lin and Kuh (1992).

6.5.2 Vector-fitting

Vector-fitting is a technique for fitting analytic rational functions to given data. Namely, $F(s)$ is approximated from $F(j\omega)$ data over a limited set of ω values. Polynomial curve-fitting is a solved problem, as it involved a single polynomial expression. Rational functions can be more difficult, as the fitting procedure may become iterative (Gustavsen & Semlyen, 1999).

Such methods may even be used to find lumped-element approximations to distributed, c-infinite impedances such as the $\sqrt{s+1}$.

6.5.3 Example Semi-inductor Approximation

The semi-inductor impedance may be approximated using a ladder network of lumped elements, leading to a rational function expression. This

approximation is detailed in Weece and Allen (2010).

Another way to realizes $\sqrt{s}$ is to use a lumped-element approximation to a uniform, semi-infinite transmission line. By setting $G = C = 0$, the remaining R and L parameters can be set to the appropriate semi-inductance value of $K = \sqrt{\frac{R}{L}}$.

6.6 The Non-simultaneous Universe

By Einstein's theory of relativity, the universe is inherently non-simultaneous. This fact suggests that the c-finite impedance captures the behavior of reality better than c-infinite impedances. This fact also suggests that in reality *all* wave systems have a causal surge impedance. Using c-finite impedances may require more mathematical modeling than using c-infinite impedances, however.

6.7 SPICE and C-Finite

The popular circuit solving computer program SPICE uses modified nodal analysis for solving circuit behavior in both the time and frequency domains. Using a quasistatic (c-infinite) model of electricity leads to the simultaneous system of equations known in SPICE as the admittance matrix (Pillage et al., 1994). Each time-step requires the solution to these equations, iteratively adjusted during each time-step to account for energy storage and other effects, such as non-linearities. As circuits become larger, computation time increases. It may become preferable to trade simultaneity with a smaller time-step. Some insight for this tradeoff comes from the finite-difference, time-domain method for solving Maxwell's equations. The finite-difference, time-domain (FDTD) method is a recursive technique; there are no simultaneous equations to solve (Yee, 1966). The cause of this recursion is due to the explicit c-finite nature of the system, where each time-step relies on local values, not global values. By combining the notion of recursive computability with SPICE, it may be possible to improve simulation accuracy and decrease computation time. The nodes may be modeled as transmission lines instead, allowing for the once large admittance matrix to decompose into

smaller, locally isolated admittance matrices. This decomposition allows for embarrassingly parallel computing, as these smaller admittance matrices are now locally independent. The wave digital filter (WDF) method described by Fettweis (1986) provides one way to accomplish this.

CHAPTER 7

THE MÖBIUS TRANSFORM AND POSITIVE REAL

The Möbius transform describes a one-to-one mapping between two complex planes. It exists purely as an abstract mathematical concept with its own properties independent of any physics. These properties make the Möbius transform useful for describing and re-expressing the PR properties of c-finite and c-infinite impedance formulas, as well as realizing alternative impedance network topologies. This chapter will discuss the mathematical properties of the Möbius transform and how to reformulate the conditions of PR under a specific Möbius transformation.

The Möbius transform also becomes useful because it emerges from the physics describing two important yet distinct c-finite concepts, the reflection coefficient and the *reflectance*, to be discussed in Chapter 8.

7.1 Möbius Transform

The general definition of a Möbius transform is given as:

$$F(w) = \frac{aw + b}{cw + d} \tag{7.1}$$

such that a, b, c, d are constants and $ad - bc \neq 0$. This formulation allows for translations, scaling, and inversions in the complex plane, and can be visualized through the aid of the Riemann sphere (Arnold & Rogness, 2008). These aspects of the Möbius transform may be found in a textbook on complex analysis such as Boas (1987, p.191) or Greenberg (1998, p.1158).

A special case of the Möbius transform involves setting $a = c = 1$ and $b = -d$. Under this condition, a single constant d effectively defines

the transform, and the transform becomes:

$$F(w) = \frac{w-d}{w+d}. \tag{7.2}$$

where d may be complex.

7.1.1 A Useful Property for Positiveness

Let F be a Möbius transform given by:

$$F = \frac{w-r}{w+r}. \tag{7.3}$$

Let $w = x + jy$ be an arbitrary complex number and let r be a real, positive constant ($r > 0$). Satisfying the following magnitude square unity bound given as:

$$FF^* \leq 1 \tag{7.4}$$

requires that $x \geq 0$ and will be proven by the following transformations. Expanding Eq. 7.4 with the real and imaginary components of w gives:

$$FF^* = \frac{x+jy-r}{x+jy+r} \cdot \frac{x-jy-r}{x-jy+r} \leq 1 \tag{7.5}$$

$$\frac{y^2+(x-r)^2}{y^2+(x+r)^2} \leq 1 \tag{7.6}$$

Since the denominator of Eq. 7.6 is always positive, the inequality may be rearranged as:

$$y^2 + (x-r)^2 \leq y^2 + (x+r)^2 \tag{7.7}$$

which simplifies to:

$$4xr \geq 0 \tag{7.8}$$

Since $r > 0$, Eq. 7.8 further simplifies to

$$x \geq 0 \tag{7.9}$$

which proves that satisfying Eq. 7.4 requires that the real part of w ($\Re w = x$) is non-negative.

7.2 Positive Real for a Möbius-Transformed Impedance

The properties detailed in Section 7.1.1 may be used to re-express the properties of PR impedance expression. Rather than using a single value w, an impedance expression $Z(s)$ may be substituted. When an impedance expression undergoes that specific Möbius transform, the output is a *Möbius-transformed impedance* given as:

$$M(s) = \frac{Z(s) - R_m}{Z(s) + R_m} \tag{7.10}$$

where R_m is an arbitrary, positive real constant. This function may be inverted to recover the impedance:

$$Z(s) = R_m \frac{1 + M(s)}{1 - M(s)}. \tag{7.11}$$

If $Z(s)$ obeys PR, then its real part is non-negative in the RHP, including the $j\omega$ axis. As a consequence, the magnitude of $M(s)$ must be bound to unity in this same region. Mathematically, this may be expressed as the $\Re Z(s) \geq 0$ if and only if $|M(s)| \leq 1$ for all $\Re s \geq 0$.

From these basic observations, the necessary and sufficient conditions for a PR rational function Möbius-transformed impedance are given by:

1. $M(s)$ is a rational function which is real for real values of s.
2. All poles are strictly in the left-half plane.
3. The magnitude is bounded to unity along the $j\omega$ axis: $|M(j\omega)| \leq 1$.

If $M(s)$ satisfies these properties, then an impedance expression may be found by using Eq. 7.11 with R_m being an arbitrary, positive constant.

The unity bound for the Möbius-transformed impedance given by Eq. 7.10 provides a necessary condition for PR, as given by the proof in the last section. As a consequence, the number of zeros must not exceed the number of poles for a Möbius-transformed impedance. If this were not the case, then the expression would diverge at $\omega = \infty$ instead of being unity bounded. The numerator and denominator polynomials of a PR impedance have non-negative coefficients and as a consequence satisfy minimum phase. The denominator of a Möbius-transformed impedance adds together these polynomials of Z, which can only keep these roots (poles) of M in the LHP.

Multiplicity of poles and zeros *is allowed* when using a Möbius-transformed impedance. This multiplicity is broken when the polynomial coefficients change during the inverse Möbius transformation, giving simple poles and zeros as required by a PR impedance.

The entire RHP, including ($\sigma = 0$), of a Möbius-transformed impedance is analytic due to all poles being constrained to the LHP. By the maximum principle, the entire RHP has its magnitude bound to unity as well. Thus $-1 \leq M(\sigma) \leq 1$, where $\sigma \geq 0$ is a real number.

For the more general case involving non-rational functions, PR for a Möbius-transformed impedance is satisfied if $m(t)$ is real-valued and the magnitude of $M(s)$ along $j\omega$ axis and within the entire right-half plane is analytic and unity-bound.

7.3 Testing for Positive Real

A property of positive real functions is that $\Re Z(j\omega) \geq 0$ for all driving frequencies ω. Satisfying $|M| \leq 1$ along the $j\omega$ axis is a necessary condition for PR. Numerically, this becomes a simple test at a finite number of points for rational function impedances. This method generalizes to non-rational expressions as well, but the rational function will be considered.

The rational function Z has finite order for its polynomials, and thus M also has finite order for its polynomials. The magnitude square of M along the $j\omega$ axis gives another rational function in the real variable ω as:

$$M(j\omega) \cdot M(-j\omega) = |M(\omega)|^2 = \frac{N(\omega)}{D(\omega)} \tag{7.12}$$

where N and D are the numerator and denominator polynomials of ω, respectively. This expression has a finite number of local minimums and maximums along ω. If all local maximums in this function along the ω axis (as well as the points at $\omega = 0$ and $\omega = \infty$) are bound to unity, then the entire function is bound to unity. All the local extrema may be found through basic calculus by setting the derivative with respects to ω to equal zero and solving.

$$\left(\frac{N}{D}\right)' = \frac{N'D - ND'}{D^2} = 0 \tag{7.13}$$

Solving this equation becomes an exercise in polynomial root-finding for the $(N'D - ND')$ polynomial. Only the real roots of this polynomial should be considered, as these correspond to the local extrema along the ω axis itself. This is where the unity bound must be satisfied. The complex roots of $|M(\omega)|^2$ are irrelevant for the purposes of finding local extrema.

Another condition to satisfy is that all the roots of the D polynomial must be complex so that no poles lie along the $j\omega$ axis of the original M function. A pole along the $j\omega$ axis means that M is *not* PR.

For non-rational functions, the local extrema test is still a valid way to limit the number of test points for the $|M|^2$ function.

7.3.1 Applications

Vector-fitting is a process of determining a rational function fit for a given set of data (Gustavsen & Semlyen, 1999). Often, the data being fitted is a PR function, but the fitting procedure may not fully preserve this property. For example, minimizing fitting error for a noisy measurement may cause a violation of PR. By using the properties of a Möbius-transformed impedance, the process of determining whether a rational function satisfies PR becomes a numerical exercise using the recipe describe in Section 7.2.

Also, randomly generating PR impedance functions becomes a simple matter. Start with a random sampling of conjugate symmetric poles and zeros in the Möbius-transformed impedance domain, such that the number of poles exceeds the number of zeros. Find the maximum value of the magnitude square along the $j\omega$ axis and then scale the rational function by the inverse of this value (or less). Inverting the Möbius-transformed impedance (by using Eq. 7.11) gives a PR rational function.

7.4 Factoring a Möbius-Transformed Impedance

A Möbius-transformed impedance may be factored into a product of Möbius-transformed impedances as shown:

$$M(s) = M_1(s)M_2(s). \tag{7.14}$$

The individual factors M_1 and M_2 functions need not satisfy the conditions described in Section 7.2. This point will be addressed later. For now, let us pursue this factorization. A Möbius-transformed impedance may be inverted to recover the underlying impedance function by using Eq. 7.11. The factored expression may be re-expressed as:

$$\frac{Z(s)-R}{Z(s)+R} = \frac{Z_1(s)-R_1}{Z_1(s)+R_1} \cdot \frac{Z_2(s)-R_2}{Z_2(s)+R_2}. \tag{7.15}$$

Solving for $Z(s)$ gives

$$Z(s) = R\frac{R_1R_2 + Z_1(s)Z_2(s)}{R_1Z_1(s) + R_2Z_2(s)} \tag{7.16}$$

This expression is equivalent to:

$$Z(s) = R\frac{\frac{Z_1(s)}{R_1}\frac{Z_2(s)}{R_2}+1}{\frac{Z_1(s)}{R_1}+\frac{Z_2(s)}{R_2}} \tag{7.17}$$

$$= R\left(\frac{\frac{Z_1(s)}{R_1}\frac{Z_2(s)}{R_2}}{\frac{Z_1(s)}{R_1}+\frac{Z_2(s)}{R_2}} + \frac{1}{\frac{Z_1(s)}{R_1}+\frac{Z_2(s)}{R_2}}\right). \tag{7.18}$$

The first term in Eq. 7.18 is of the form of a parallel combination of impedances:

$$\frac{1}{\frac{1}{Z_1}+\frac{1}{Z_2}} = \frac{Z_1Z_2}{Z_1+Z_2} \tag{7.19}$$

The second term in Eq. 7.18 is of the from of the dual of a series combination of impedances, or a parallel combination of admittances:

$$\frac{1}{Z_1+Z_2} = \frac{1}{\frac{1}{Y_1}+\frac{1}{Y_2}} = \frac{Y_1Y_2}{Y_1+Y_2}. \tag{7.20}$$

From a network topology point of view, the factoring of a Möbius-transformed impedance describes a parallel combination of Z_1 and Z_2 in series with the dual of the series combination of Z_1 and Z_2. Alternatively, the dual may be considered a parallel combination of the *admittances*. Thus, an impedance network $Z(s)$ may be factored to produce a separate network described as:

$$Z(s) = R\left(\frac{Z_1(s)}{R_1}||\frac{Z_2(s)}{R_2} + \frac{Y_1(s)}{G_1}||\frac{Y_2(s)}{G_2}\right) \tag{7.21}$$

where $Y = 1/Z$ and $G = 1/R$. This result generalizes to all impedances networks, including those not described by rational polynomials.

7.4.1 Non-Positive Real Factorizations

Not every rational function can be factored such that its products satisfy unity-bound magnitude along the $j\omega$ axis. Inverting a non-PR Mobius-transformed impedance gives an expression for a non-PR impedance, meaning that the impedance network contains *active elements*. Combining these separate networks as described by Eq. 7.21 will still give an overall passive impedance. This is true as a consequence of the mathematics, and physically it corresponds to one active network being offset by its dual active network.

7.4.2 Network Topology with a Gyrator

The gyrator is an anti-reciprocal, linear two-port device described by Tellegen (1948). It effectively swaps the voltage and current, allowing the dual of a network to be realized without changing the original network. The ABCD matrix for a gyrator with gyration resistance R is given as:

$$T = \begin{bmatrix} 0 & R \\ \frac{1}{R} & 0 \end{bmatrix} \tag{7.22}$$

Two identical gyrators cascaded creates a unity transformer, as $TT = I$, the identity matrix. If the two gyrators had different gyrator resistances, R_1 and R_2, then the cascade of these two non-identical gyrators gives a transformer with a turns ratio of $a = \frac{R_2}{R_1} = \frac{N_1}{N_2}$, where N_1 and N_2 are the turns on the primary and secondary windings, respectively (Pai, 2003).

The topology described in Eq. 7.21 can be realized by using a unity gyrator to realize the dual. Figure 7.1 shows the schematic of this factored network. The once simple input impedance network Z may be expanded to this network. The impedances Z_1 and Z_2 are rescaled by the constants R_1 and R_2 used in each Möbius transformation.

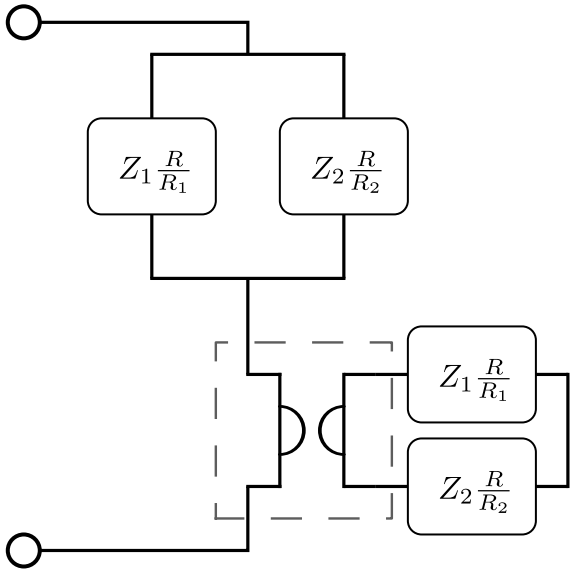

Figure 7.1: Resultant network when factoring the Möbius-transformed impedance expression using a unity gyrator, indicated by the dashed border.

7.4.3 All-pass and Minimum Phase Factorization

One such factorization that is guaranteed is the all-pass (AP) and minimum-phase (MP) factorization. This factorization has the useful physical interpretation of a lossless network (AP) coupled to a lossy network (MP). It may be possible that $M(s)$ yields a factorization such that either the AP or MP component is unity magnitude, and this is still valid.

7.4.4 Degenerate Factorization

It may be possible that one of the factors is degenerate, i.e. $M_1(s) = \pm 1$. This is an acceptable result, as the mathematics of the Möbius-transformed impedance factorization and realization still hold. When the factorization M_1 term approaches unity magnitude, then two possible interpretations of Z_1 exist. One interpretation is that the factored impedance approaches positive, real infinity for $M_1(s) = 1$:

$$\lim_{Z_1 \to \infty} \frac{Z_1(s) - R_1}{Z_1(s) + R_1} = 1 \tag{7.23}$$

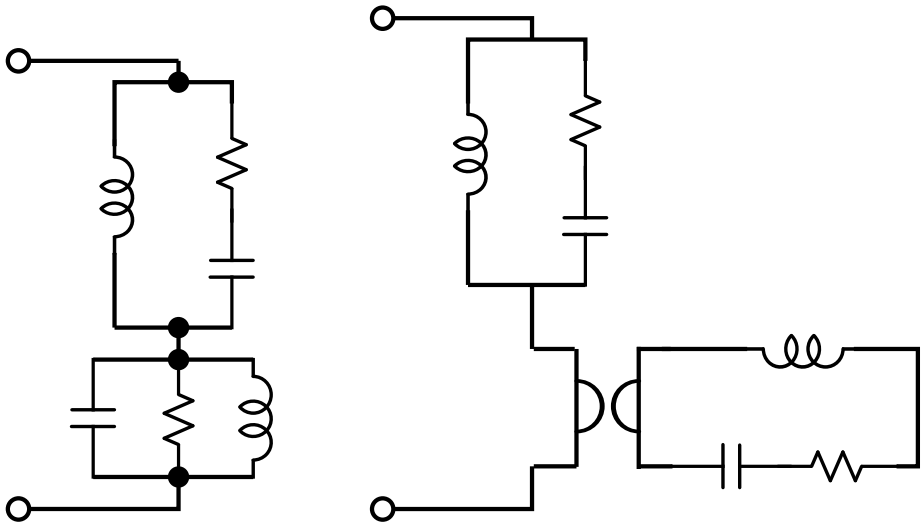

(a) Simple network. (b) Same network, but with a gyrator.

Figure 7.2: Impedance network will all elements of unity value: 1, s, 1/s

or the factored impedance approaches zero for $M_1(s) = -1$:

$$\lim_{Z_1 \to 0} \frac{Z_1(s) - R_1}{Z_1(s) + R_1} = -1 \tag{7.24}$$

When either limit is taken in the context Eq. 7.21, the end result is that the entire impedance is a function of just the second term, i.e. $Z = R\frac{Z_2}{R_2}$.

7.4.5 Example Factorization

Consider the following impedance formula:

$$Z(s) = \frac{s^2 + 2s}{s^2 + s + 1} \tag{7.25}$$

Equation 7.25 describes a network with all capacitors, inductors, and resistors with unity value as shown in Fig. 7.2, as well as its realization with a gyrator from Fig. 7.1. A partial fraction expansion (and residue) of Eq. 7.25 gives:

$$Z(s) = 1 + \frac{s - 1}{s^2 + s + 1} \tag{7.26}$$

$$= 1 + \frac{\frac{-j\sqrt{3}}{3}}{s - \left(\frac{-1-j\sqrt{3}}{2}\right)} + \frac{\frac{j\sqrt{3}}{3}}{s - \left(\frac{-1+j\sqrt{3}}{2}\right)} \tag{7.27}$$

This impedance given in Eq. 7.25 has the following inverse Laplace transform:

$$z(t) = \delta(t) + e^{-t/2}\left(\cos\left(t\frac{\sqrt{3}}{2}\right) - \sqrt{3}\sin\left(t\frac{\sqrt{3}}{2}\right)\right)u(t) \tag{7.28}$$

The delta function is not surprising, as it is the instantaneous, lossy resistance seen at time $t = 0$. At that instance, the capacitors act as short-circuits and the inductors act as open-circuits. The closed path contains the instantaneous resistance of the circuit – the resistor in the top part of the circuit.

The Möbius-transformed impedance expression for Eq. 7.25, using Eq. 7.10, and setting $R_m = 1$ becomes:

$$M(s) = \frac{Z(s) - 1}{Z(s) + 1} \tag{7.29}$$

$$= \frac{s - 1}{2s^2 + 3s + 1} \tag{7.30}$$

$$= \underbrace{\left(\frac{s-1}{s+1}\right)}_{\text{all-pass}} \underbrace{\left(\frac{1}{2s+1}\right)}_{\text{minimum-phase}} . \tag{7.31}$$

7.5 Poles and Zeros of RLC Impedance Networks

Foster's reactance theorem and Cauer's extensions offer a restriction to the geometrical placement of poles and zeros in $Z(s)$ for two-type networks. The three-type RLC network does not have a known geometrical configuration for its poles and zeros other than the placement satisfying positive real.

Assume that

$$Z(s) = \frac{N(s)}{D(s)} \tag{7.32}$$

Then the Möbius-transformed impedance may be expressed as:

$$M(s) = \frac{Z(s) - R_m}{Z(s) + R_m} = \frac{N(s) - R_m D(s)}{N(s) + R_m D(s)} \tag{7.33}$$

by distributing $D(s)$, and then R_0 for the later purposes of conceptualizing the extreme limits of R_m. Note that the choice of R_m shifts the poles and zeros in the $M(s)$ domain.

In the limit as R_m approaches zero, the coefficients of the numerator and

denominator polynomials approach that of $N(s)$, thus the poles and zeros of $M(s)$ converge to the locations of the zeros in the $Z(s)$ domain. The information about the zeros in $Z(s)$ leak into $M(s)$ while still satisfying magnitude unity-bound along the $j\omega$ axis. In the limit as R_0 approaches infinity, the coefficients of the polynomials approach that of $D(s)$, thus the poles and zeros of $M(s)$ converge to the locations of the poles in the $Z(s)$ domain. This numerical trick could, in theory, lend some insight into the restrictions of poles and zeros in $Z(s)$.

CHAPTER 8

REFLECTANCE AND THE REFLECTION COEFFICIENT

The Möbius transform described in Chapter 7 can be used to describe two important c-finite concepts: the *reflection coefficient* and the *reflectance*. Both the reflection coefficient and reflectance satisfy the mathematical properties of a Möbius-transformed impedance. However, these two concepts arise from physically distinct systems. This chapter will explore the two concepts and how the Möbius transformation arises from their physical meaning.

8.1 Reflection Coefficient

The reflection coefficient is typically expressed as:

$$\Gamma(s) = \frac{Z_{\text{load}}(s) - Z_{\text{source}}(s)}{Z_{\text{load}}(s) + Z_{\text{source}}(s)} \tag{8.1}$$

where z_{load} and z_{source} are the characteristic impedances (see Eq. 4.5) of the media. In general, both the load and source terms can be functions of s. Another way to express the reflection coefficient is by normalizing its source impedance:

$$\Gamma(s) = \frac{\frac{Z_{\text{load}}(s)}{Z_{\text{source}}(s)} - 1}{\frac{Z_{\text{load}}(s)}{Z_{\text{source}}(s)} + 1} \tag{8.2}$$

Such a normalization of the reflection coefficient allows the use of a Smith chart for analysis (Rao, 2004), directly expressed as a Möbius transform from Eq. 7.2, with the single complex function as $w = Z_{load}(s)/Z_{source}(s)$.

The reflection coefficient arises from satisfying boundary conditions between two wave-propagating media. The boundary conditions require continuity in the total voltage and net current. These quantities may be expressed in terms of incident V^+ and reflected V^- waves. Figure 8.1 depicts

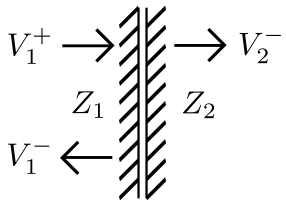

Figure 8.1: Incident and reflected waves at a boundary for describing a reflection coefficient.

the incident and reflected waves at a boundary of two coupled media with characteristic impedance $Z_1 = Z_{source}$ and $Z_2 = Z_{load}$. An incident wave V_1^+ interacts with the boundary, causing a reflected wave V_1^- and a transmitted wave V_2^-. The ratio of the reflected to the incident wave is the reflection coefficient given as:

$$\Gamma = \frac{V_1^-}{V_1^+} \tag{8.3}$$

The total voltage V and net current I at each side of the boundary can be expressed as:

$$V_1 = V_1^+ + V_1^- \tag{8.4}$$

$$I_1 = \frac{1}{Z_1}\left(V_1^+ - V_1^-\right) \tag{8.5}$$

$$V_2 = V_2^- \tag{8.6}$$

$$I_2 = \frac{1}{Z_2}\left(-V_2^-\right) \tag{8.7}$$

where the direction of the current is toward the boundary (same as V^+). The boundary conditions to satisfy become:

$$V_1 = V_2 \tag{8.8}$$

$$I_1 = -I_2. \tag{8.9}$$

Combining all these equations and solving the the ratio of V_1^-/V_1^+ gives Eq. 8.1, where medium 1 is the source and medium 2 is the load.

8.2 Reflectance

The reflectance describes wave propagation of a c-finite impedance $Z(s)$ as:

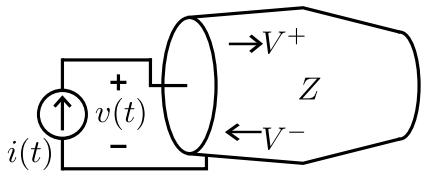

Figure 8.2: Incident and reflected waves at an ideal current source for describing the reflectance of the c-finite impedance $Z(s)$.

$$\mathcal{G}(s) = \frac{Z(s) - R_0}{Z(s) + R_0}, \tag{8.10}$$

where R_0 is the *surge impedance* of the c-finite $Z(s)$. The boundary condition at the impedance input is an *ideal current source* (i.e. one which has no source impedance). Figure 8.2 shows the physical configuration of the ideal current source, a c-finite impedance, and the inbound and outbound waves at the input boundary.

Since the reflectance is of the form of a Möbius-transformed impedance, $Z(s)$ can be recovered from $\mathcal{G}(s)$ by using Eq. 7.11, with $R_m = R_0$. The origin of a reflectance arises from re-expressing Ohm's law using the reflectance instead of the impedance:

$$V(s) = I(s)\, Z(s) \tag{8.11}$$

$$= I(s)\, R_0 \frac{1 + \mathcal{G}(s)}{1 - \mathcal{G}(s)} \tag{8.12}$$

These terms may be re-arranged:

$$V(s)\,(1 - \mathcal{G}(s)) = R_0\,(1 + \mathcal{G}(s))\, I(s) \tag{8.13}$$

$$V(s) = R_0 I(s) + R_0 I(s)\mathcal{G}(s) + V(s)\mathcal{G}(s) \tag{8.14}$$

Taking the inverse Laplace transform yields:

$$v(t) = R_0 \overbrace{i(t)}^{\text{input}} + R_0 \overbrace{\left(\int_{0^-}^{t} i(\tau)\, g(t-\tau) d\tau \right)}^{\text{feedforward}} + \overbrace{\int_{0^-}^{t} v(\tau)\, g(t-\tau) d\tau}^{\text{feedback}} \tag{8.15}$$

This convolutional relationship takes the form of a Fredholm integral equation, as the output $v(t)$ depends on its previous values, given by the feedback convolutional term.

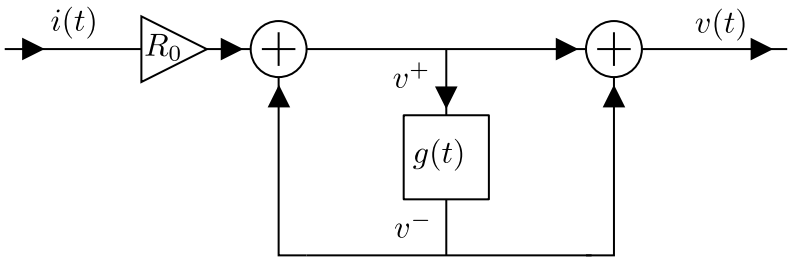

Figure 8.3: Signal flow diagram for a reflectance in Fig. 8.2 and the time domain Eq. 8.15.

8.3 Reflectance Signal Flow Diagram

A signal flow diagram may be constructed to model this reflectance system from Eq. 8.15, as shown in Fig. 8.3. The input signal $i(t)$ feeds into the system through the surge impedance R_0 which directly reaches the output $v(t)$. In the middle exists a convolutional relationship with $g(t)$ which acts as both the feedforward and feedback signal paths. For those familiar with digital signal processing, Eq. 8.15 may be expressed in direct form I, which then can be re-arranged to give direct form II, which is the form given in Fig. 8.3.

8.3.1 Reflectance Computability

In order for the reflectance system to be computable, the feedback portion must not respond instantaneously to an input. This is required to assure that the system does not become simultaneous. Therefore the kernel $g(t)$ must not have a Dirac delta singularity at time $t = 0$. Avoiding this singularity *requires* choosing the surge impedance R_0 as the R_m parameter in Eq. 7.10. Thus, only c-finite impedances may be expressed as time-domain reflectances, due to the computability (non-simultaneous) constraint.

8.4 Physical Interpretation of Reflectance

All c-finite impedances have a surge impedance, which must be used as the constant parameter R_m in the Möbius-transformed impedance. Since the c-finite impedance supports wave propagation, one can interpret the signal flow diagram in terms of traveling waves within the impedance structure. A

current impulse entering the system at $t = 0$ launches a forward-traveling wave into the impedance structure. This wave is then reflected back to the input through the convolutional relationship with $g(t)$. The boundary condition at the input causes this inbound wave to be fully reflected back into the impedance structure, as modeled by the feedback portion of the signal flow diagram, modeled as the same convolution with $g(t)$. Thus the waves traveling away from the input boundary are $v^+(t)$, and the reflected waves returning to the input boundary are $v^-(t)$. The choice of voltage or current wave variables is arbitrary.

The reflectance concept offers an alternative method for expressing the time-domain convolutional relationship of Ohm's law, once one fully embraces the wave nature of the impedance.

The instantaneous power is given as the product of the voltage and current:

$$p(t) = i(t) \cdot v(t) \tag{8.16}$$

which are the input and output signals of Fig. 8.3. The reflectance and impedance of a physical device are related to its power properties. The ideal current source drives the impedance structure, delivering energy to and absorbing energy from the impedance structure.

8.5 Contrasting the Reflectance with the Reflection Coefficient

The frequency-domain expression for the reflectance closely resembles that of a reflection coefficient, since both are superficially in the form of a Möbius-transformed impedance. However, due to physical considerations, they are fundamentally different concepts. A reflectance is a property of a single c-finite impedance and is fully consistent with Maxwell's equations, whereas a reflection coefficient describes wave reflections of two coupled media at the boundary. Measuring a reflection coefficient requires a Norton (or Thevenin) source with its own positive real source impedance connected to a PR load impedance. The reflectance requires an ideal current (or voltage) source connected to the c-finite impedance. Equation 8.17 displays both formulas,

side-by-side for comparison.

$$\mathcal{G}(s) = \frac{Z(s) - R_0}{Z(s) + R_0} \qquad \Gamma(s) = \frac{z_{\text{load}}(s) - z_{\text{source}}(s)}{z_{\text{load}}(s) + z_{\text{source}}(s)} \tag{8.17}$$

The surge impedance R_0 is a unique property of a c-finite impedance $Z(s)$. The time-domain reflectance consists entirely of a residual response without an initial singularity. The reflection coefficient arises from satisfying boundary conditions between two wave propagating media with characteristic impedances z_{load} and z_{source}. The reflection coefficient allows both z_{load} and z_{source} to be functions of s, whereas the reflectance, as a consequence of the Möbius transformation of $Z(s)$, requires that R_0 is a real constant. This is a subtle yet critically important distinction. The reflectance and reflection coefficient, despite both involving wave propagation, are fundamentally distinct. This distinction is one of the most important conclusions of this thesis.

8.6 Reflectance Examples

Several examples of a reflectance will be considered. Additional examples of non-uniform transmission lines may be found in Appendix B.

8.6.1 Lossless Transmission Line Stubs

The transmission lines described in Section 5.3 offered the time- and frequency-domain expressions for transmission line stubs with open (capacitive) and short (inductive) terminating conditions. Discrete-time filter realizations were given in Section 5.4. There exists a parallel between the continuous- and discrete-time realization, because a tapped delay line implements discrete convolution. These two systems have extremely simple reflectance formulations for continuous time.

The capacitor stub impedance, given in Eqs. 5.3 and 5.5, has equivalent frequency- and time-domain expressions as:

$$\mathcal{G}(s) = e^{-sT} \tag{8.18}$$

$$g(t) = \delta(t - T) \tag{8.19}$$

The time-domain reflectance offers a simple explanation with respect to the signal flow diagram in Fig. 8.3. An initial current impulse enters, manifesting as a voltage impulse. This impulse is then convolved with $g(t)$, causing a delayed impulse to feed back into the system as well as feed forward. The sum of the feedback and feedforward paths gives twice-unity impulses. The feedback impulse causes this periodic train of twice-unity impulses to continue indefinitely, as expressed in Eq. 5.5.

The inductor stub impedance, given in Eq. 5.6 and 5.8, has equivalent frequency- and time-domain expressions as:

$$\mathcal{G}(s) = -e^{-sT} \tag{8.20}$$

$$g(t) = -\delta(t - T) \tag{8.21}$$

This is very similar to the capacitor signal flow, but the negative $\delta(t - T)$ causes the alternative sign behavior for the impulses as expressed in Eq. 5.8.

8.6.2 Padé Approximation

Reflectance formulations can also be expressed using a Padé approximation, as long as the denominator order exceeds the numerator. The exponential reflectance given in Eq. 8.18 has the following Taylor series expansion:

$$e^{-s} = 1 - \frac{s^1}{1!} + \frac{s^2}{2!} - \frac{s^3}{3!} + \frac{s^4}{4!} - \frac{s^5}{5!} + \frac{s^6}{6!} + ... \tag{8.22}$$

$$= \sum_{n=0}^{\infty} (-1)^n \frac{s^n}{n!} \tag{8.23}$$

These coefficients of this expansion may be used to compute the Padé approximation (Press et al., 2007). Example Padé approximations using the first three terms are given here, with increasing denominator polynomial

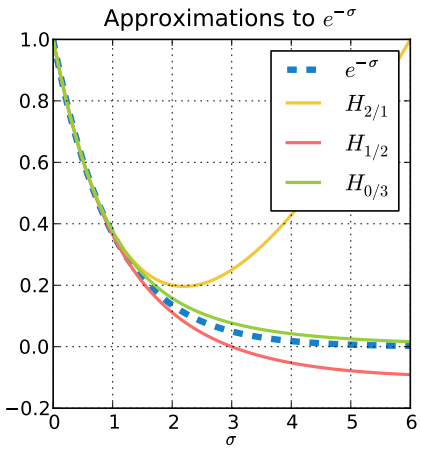

Figure 8.4: Approximations to $e^{-\sigma}$ following Eqs. 8.24 to 8.26

orders:

$$H(s) = e^{-s} \approx \frac{\frac{1}{6}s^2 - \frac{2}{3}s + 1}{\frac{1}{3}s + 1} = H_{2/1} \tag{8.24}$$

$$e^{-s} \approx \frac{-\frac{1}{3}s + 1}{\frac{1}{6}s^2 + \frac{2}{3}s + 1} = H_{1/2} \tag{8.25}$$

$$e^{-s} \approx \frac{1}{\frac{1}{6}s^3 + \frac{1}{2}s^2 + s + 1} = H_{0/3} \tag{8.26}$$

Figure 8.4 shows various Padé approximations for different numerator and denominator polynomial orders, plotted along the real σ axis. Having a higher numerator order causes the approximation to diverge for larger values of σ.

The magnitude and phase of the Padé approximation of the first 20 Taylor series coefficients are shown against the original function in Fig. 8.5(a). The phase of the approximation is linear up to 20 radians and then approaches an asymptote at higher frequencies. Despite e^{-s} being lossless, the proper Padé approximation for a reflectance gives a lossy system at higher frequencies. The poles and zeros of one such proper Padé approximation are given in Fig. 8.5(b).

To preserve the lossless nature of the reflectance one must use an all-pass filter configuration for the poles and zeros, meaning that the rational function must be equi-order. Such a formulation no longer describes a proper reflectance due to its initial singularity in the time-domain expression; it is a simple Möbius-transformed impedance. Figure 8.6 shows the magnitude,

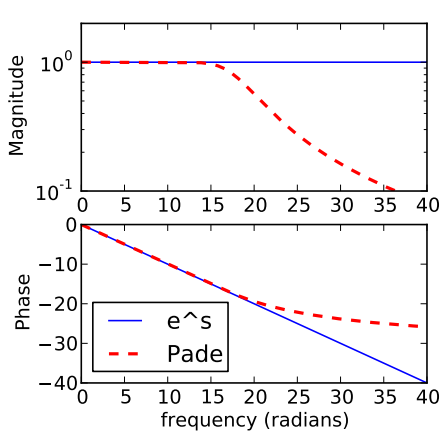

(a) Magnitude and phase of e^{-s} and Padé approximation

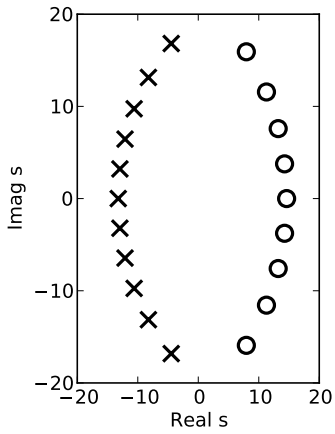

(b) 11 poles and 9 zeros of Padé approximation

Figure 8.5: Padé approximation to e^{-s} and pole/zero pattern. This is a valid reflectance.

phase, and all-pass pole/zero plot for the equi-order Padé approximation.

8.6.3 Uniform Transmission Line Example

The semi-infinite, uniform transmission line described in Section 4.3 gives the frequency- and time-domain expressions for the input impedance. The Möbius impedance for this system may be expressed as:

$$\mathcal{G}(s) = \frac{Z(s) - R_0}{Z(s) + R_0} = \frac{\sqrt{\frac{R+sL}{G+sC}} - R_0}{\sqrt{\frac{R+sL}{G+sC}} + R_0} \tag{8.27}$$

where $R_0 = \sqrt{\frac{L}{C}}$ is the surge impedance. Rather than directly use the surge impedance in the formulation of $\mathcal{G}(s)$, the initial singularity theorem will be used to prove that avoiding an initial singularity requires setting R_0 to the true surge impedance. Taking the limit as s approaches infinity along the real σ axis gives:

$$\lim_{\Re s \to +\infty} \mathcal{G}(s) = \frac{\sqrt{\frac{L}{C}} - R_0}{\sqrt{\frac{L}{C}} + R_0} \tag{8.28}$$

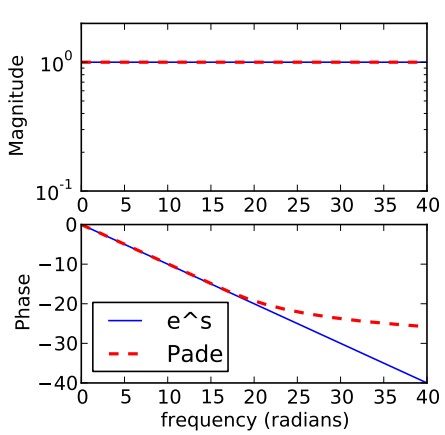

(a) Magnitude and phase of e^{-s} and Padé approximation

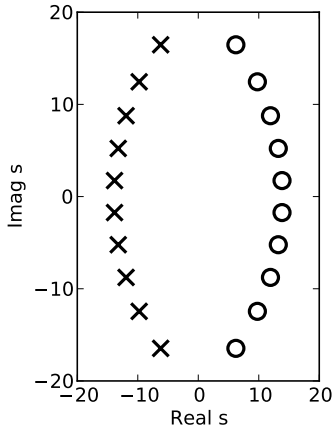

(b) 10 poles and 10 zeros of Padé approximation

Figure 8.6: Padé approximation to e^{-s} and all-pass pole/zero pattern. This is not a valid reflectance due to its initial time-domain singularity.

Therefore, in order to avoid an initial singularity in $g(t)$, the constant in the Möbius impedance transform must be set to the surge impedance: $R_0 = \sqrt{\frac{L}{C}}$.

Despite $g(t)$ lacking an initial singularity, the time-domain reflectance may still have an initial value. By the initial value theorem, this value may be found:

$$\lim_{\Re s \to +\infty} s\,\mathcal{G}(s) = \frac{1}{4}\left(\frac{R}{L} - \frac{G}{C}\right) \tag{8.29}$$

Having a non-zero initial value does not violate the computability of the reflectance signal flow diagram from Fig. 8.3. The convolutional operator at time $t = 0$ evaluates to zero, since there is no initial singularity and the bounds of the integral are equal, which makes the regular integral evaluate to zero.

The time-domain expression for $g(t)$, using Table A.1, is:

$$g(t) = \frac{1}{t} e^{-\frac{1}{2}(\alpha+\beta)\,t} I_1\left(\frac{1}{2}(\alpha-\beta)\,t\right) u(t) \tag{8.30}$$

where $\alpha = R/L$ and $\beta = G/C$. The limit as $t \to 0$ of $g(t)$ gives the result from Eq. 8.29.

The time-domain reflectance in Eq. 8.30 is a simpler expression than the equivalent time-domain impedance as given by Eq. 4.14, reprinted here for

convenience.

$$z(t) = \overbrace{\sqrt{\frac{L}{C}}\delta(t)}^{\text{surge}} + \overbrace{\frac{1}{2}\sqrt{\frac{L}{C}}\,(\alpha-\beta)\,e^{\frac{-(\alpha+\beta)t}{2}}\left[I_1\left(\frac{1}{2}(\alpha-\beta)t\right)+I_0\left(\frac{1}{2}(\alpha-\beta)t\right)\right]u(t)}^{\text{residual}}$$

CHAPTER 9

CONCLUSIONS

Impedance exists equally as both a time- and frequency-domain concept, despite the popular preference toward the frequency-domain interpretation. The properties of an impedance in both time and complex frequency domains give insight into impedance. The very convenient and powerful rational function representation is limited in how it captures the physics of an impedance.

The rational function expression for an impedance, while a convenient model for impedance, has fundamental limitations in its time-domain formulation. Brune's positive real (PR) formulation proves that rational function impedance formulations have a realization as a lumped-element network, all of which are non-physical, quasistatic Padé approximations. These formulations, while mathematically convenient, are an incomplete interpretation of the impedance concept.

Including wave propagation into the impedance model has implications in both its time- and frequency-domain properties. All impedances describing wave propagating systems are of the form described in Eq. 1.1:

$$z(t) = R_0\delta(t) + z_{res}(t)u(t) \ ,$$

where R_0 is the instantaneous surge impedance, representing the initial energy entering as wave into the impedance structure, but not (necessarily) as a loss. The z_{res} term models the reflections returning to the input boundary, which are then reflected back into the impedance structure by an ideal source. The frequency-domain implications for a c-finite impedance, by the initial singularity theorem, require that the limit as $\Re s \to +\infty$ approach a finite positive constant.

Equi-order rational functions may have a dual interpretation as a c-finite impedance, but the initial Dirac delta must represent an energy loss term as

a consequence of Foster's reactance theorem (Section 6.2). Thus, equi-order rational functions may be appropriate for modeling radiation impedance when losses (energy radiating away) are expected.

A purely lossy component, i.e. a resistor, has several realizations. It may be realized by quasistatic approximations, and it may be realized by careful selection of transmission line parameters (Sections 4.3 and 4.4. A pure loss can be realized as a semi-infinite line with wave propagation (c-finite) or a purely lossy line with no distributive reactance (c-infinite). Its most interesting realization uses a lossless, semi-infinite transmission line, where the initial wave entering into the transmission line continues forever toward $x = +\infty$. For all intents and purposes, this energy is lost because it never returns.

A c-finite impedance network describes a system that is spatially non-simultaneous by its very nature of having delay due to wave propagation. This is consistent with Maxwell's equations. Non-simultaneity also permits recursive modeling of these c-finite systems. A c-infinite impedance network prohibits wave propagation, describing a simultaneous system where all parts interact simultaneously. Such a system requires solutions to simultaneous equations. Lumped-element networks, as well as distributed networks without wave propagation (like those modeled with the diffusion equation), fall under the c-infinite category. Mixing these two impedance classes creates models of locally simultaneous and non-simultaneous systems.

Working with impedance exclusively in the frequency domain has obscured this fundamental distinction between c-finite and c-infinite impedances. As a consequence, the physical assumptions underlying each network become hidden. These assumptions have implications concerning accuracy when modeling in both the frequency and time domain. For example, lumped-element approximations to transmission lines may be useful over a limited frequency range, but this approximation's time-domain properties will be very different from the c-finite model.

The c-finite and c-infinite classes may be used to approximate each other by various mathematical transformations or curve-fitting. Padé approximations and vector fitting are used to approximate c-finite and irrational c-infinite impedances as c-infinite rational functions. The c-infinite rational functions may be approximated as c-finite via the bilinear transformation. These discrete-time impedances have a continuous time realization as a periodic

sequence of weighted Dirac delta functions.This interlinking between c-finite and c-infinite classes may be useful for arriving at models that possess reasonable time- and frequency-domain properties.

A bilinear transformation of a PR impedance function gives a discrete-time expression for an impedance, which allows for physical interpretations of discrete filters in terms of properties of PR. These discrete-time impedance systems, like their continuous-time counterparts, are minimum phase and have causal and stable inverses.

The properties of positive real as given by Brune applied to rational function expressions, but can be generalized to non-rational expression as well. The PR properties have an equivalent re-expression in the Möbius-transformed impedance domain, where an impedance function transforms according to Eq. 7.10:

$$M(s) = \frac{Z(s) - R_m}{Z(s) + R_m}$$

The primary conditions for PR in the Möbius-transformed impedance domain is a unity-bound magnitude along the entire $j\omega$ axis, and all poles must exist in the LHP. This allows for a simple numerical test for whether or not a given rational function satisfies PR.

The Möbius-transformed impedance transformation can be factored into a product of two Möbius-transformed impedances and has a network realization of a parallel combination of the two networks in series with the dual of the two networks in series (Eq. 7.21). This dual network realization may involve a gyrator.

A special case of the Möbius impedance, called reflectance, applies to all c-finite impedances. Reflectance allows for an alternative realization of Ohm's law in the time domain, where outbound and inbound waves are fully explained by reflectance $\mathcal{G}$ and the surge impedance R_0. Reflectance offers a more physical interpretation of the c-finite impedance by fully embracing the wave-nature of the impedance structure at the input boundary.

Reflectance shares a similar mathematical formulation to that of a reflection coefficient. However, a reflection coefficient allows both z_{load} and z_{source} to be functions of s, whereas reflectance, as a consequence of being a Möbius transformation, requires that R_0 always be a constant. This is a very subtle, yet critically important distinction. Thus, the reflectance and reflection coefficient are *very* different.

It seems that now is a good time to move away from the quasistatic approximation and move into the physical c-finite world as described by reflectance. This emphasis on reflectance is keeping with the high-bandwidth world we live in (reflectance captures high-bandwidth features). Using reflectance would also be consistent with modern digital signal processing and its emphasis on time-domain sampled data systems. Such a scheme would allow for digital impedance, consistent with modern wave digital filter concepts (Fettweis, 1986).

The core message of this thesis can be summarized with the following:

1. Impedance models exist in the time and frequency domain.

2. Impedance may include wave propagation (c-finite) or not (c-infinite).

3. Reflectance offers a unique formulation of c-finite impedances.

The rational function formulation, embrace by Brune in his formulation of PR, only captures a tiny subset of phyical impedances. Thus, the Brune impedance has greatly limited our view of physical reality.

APPENDIX A

THE LAPLACE TRANSFORM

Heaviside's operational calculus helped in defining an electrical impedance, despite its initial lack of a formal mathematical proof. His calculus did not detract from its utility in solving electromagnetic problems and was adopted despite objection from mathematicians. Bromwich later showed an equivalence with the Laplace transform, which placed Heaviside's mathematical intuition on a firm mathematical foundation (Lützen, 1979). The Laplace transform framework has since superseded some of Heaviside's original mathematics for describing impedance.

The Laplace transform is defined as:

$$F(s) = \int_{0^-}^{\infty} f(t)e^{-st}dt \tag{A.1}$$

The lower bound of the integral 0^- explicitly includes an initial Dirac $\delta^{(n)}(t)$ singularity that may exist at $t = 0$, as well as any derivatives. The lower bound of the integral approaches zero from the negative side of the number line which may be interpreted as a pre-initial condition. Lundberg, Miller, and Trumper (2007) offer an excellent overview of these subtleties concerning the lower bound of the Laplace transform. Some of their results will be revisited here.

A.1 Initial Singularity Theorem

According to Lundberg et al. (2007),"the initial-singularity theorem asserts that F(s) is asymptotic, as s increases through the real numbers, to a polynomial that carries information about the singularity of $f(t)$ at $t = 0$."

The Laplace transform of a Dirac singularity, and its derivatives, may be

expressed as:

$$\mathcal{L}_{-}\left(\delta^{(n)}(t)\right) = s^n \tag{A.2}$$

A function with initial singularities may be expressed as:

$$F(s) = \widetilde{F}(s) + \sum_{n=1}^{N} a_n s^n \tag{A.3}$$

where "the function $\widetilde{F}(s)$ converges to zero in the limit $\Re s \to +\infty$." Subtracting a properly weighted polynomial in s will yield $\widetilde{F}(s)$ which has no initial singularity.

A.1.1 Delayed singularities

Delayed singularities have the transform

$$\mathcal{L}\left(\delta^{(n)}(t-a)\right) = s^n e^{-sa} \tag{A.4}$$

These singularities that occur after $t = 0$ have an e^{-sa} factor, which causes these delayed singularities to approach zero value in the limit as $\Re s \to +\infty$.

A.2 Initial Value Theorem

The initial value theorem reveals the time-domain value at $t = 0^+$. Using $\widetilde{F}(s)$ as defined in Section A.1, the initial value theorem is given as:

$$\lim_{\Re s \to +\infty} s\widetilde{F}(s) = \widetilde{f}(0^+) \tag{A.5}$$

A.3 Laplace Transform Identities

Campbell and Foster (1942) provided a table of useful irrational inverse Laplace transforms (as well as many other forms). Some of these inversions are reproduced here in Table A.1. Campbell and Foster's p variable means the same as s, and g means the same as t, and each has been substituted accordingly in this partial reproduction. The left column reproduces the identity number, as given in the original text.

Table A.1: Table of select inverse Laplace transform identities from Campbell and Foster (1942).

No.	H(s)	Coefficient h(t)
503	$s^{\frac{1}{2}}$	$-\frac{1}{2\pi^{\frac{1}{2}}t^{\frac{3}{2}}}$
522	$\frac{1}{s^{\frac{1}{2}}}$	$\frac{1}{(\pi t)^{\frac{1}{2}}}$
526	$\frac{1}{(s+\rho)^{\frac{1}{2}}}$	$\frac{1}{(\pi t)^{\frac{1}{2}}}e^{-\rho t}$
530.5	$(s+\rho)^{\frac{1}{2}}-(s+\sigma)^{\frac{1}{2}}$	$\frac{1}{2\pi^{\frac{1}{2}}t^{\frac{3}{2}}}(e^{-\sigma t}-e^{-\rho t})$
559.2	$\frac{(s+\rho)^{\frac{1}{2}}-(s+\sigma)^{\frac{1}{2}}}{(s+\rho)^{\frac{1}{2}}+(s+\sigma)^{\frac{1}{2}}}$	$\frac{1}{t}e^{-\frac{1}{2}(\rho+\sigma)t}I_1\left(\frac{1}{2}(\rho-\sigma)t\right)$
561.0	$\left(\frac{s+\rho}{s+\sigma}\right)^{\frac{1}{2}}-1$	$\frac{1}{2}(\rho-\sigma)e^{-\frac{1}{2}(\rho+\sigma)t}\left[I_1\left(\frac{1}{2}(\rho-\sigma)t\right)+I_0\left(\frac{1}{2}(\rho-\sigma)t\right)\right]$

APPENDIX B

NON-UNIFORM TRANSMISSION LINES

This supplement gives some results for non-uniform lines with electrical and acoustical interpretations.

B.1 Spherical Radiator Derivation

The radiation impedance of a spherical radiator can be derived following the steps outlined in Kinsler et al. (2000, p.127). These steps will be reproduced partially, but in enough detail to warrant a full derivation.

Quoting from Kinsler:

> The wave equation for spherically symmetric pressure fields is then
>
> $$\frac{\partial^2 p}{\partial r^2} + \frac{2}{r}\frac{\partial p}{\partial r} = \frac{1}{c^2}\frac{\partial^2 p}{\partial t^2}$$
>
> ... If the product rp in this equation is considered as a single variable, the equation [has] the general solution
>
> $$p = \frac{1}{r} f_1(ct - r) + \frac{1}{r} f_2(ct + r)$$
>
> for all $r > 0$...
>
> The most important diverging spherical waves are harmonic. Such waves are represented in complex form by
>
> $$p = \frac{A}{r} e^{j(\omega t - kr)}$$

In the equations, A denotes the complex amplitude of the pressure wave found by satisfying the boundary condition at the surface of the radiator. The $e^{j(\omega t)}$ term is a phasor. The partical velocity $\overrightarrow{u}$ relates to the pressure

by Kinsler's Eq. 5.4.10:

$$\rho_0 \frac{\partial \overrightarrow{u}}{\partial t} = -\nabla p$$

Solving for $\overrightarrow{u}$ gives Kinsler's Eq. 5.11.8:

$$\overrightarrow{u} = \hat{r}\left(1 - \frac{j}{kr}\right)\frac{p}{\rho_0 c}$$

Taking the ratio of p and $\overrightarrow{u}$ requires some manipulation of the vector in order to properly represent the specific acoustic impedance. This leads to:

$$Z = \rho_0 c \frac{kr}{\sqrt{1+(kr)^2}} e^{j\theta_a}$$

where $\cot\theta_a = kr$. By a geometric argument using the Pythagorean theorem, with sides 1, kr, and $\sqrt{1+k^2r^2}$, the ratio can be expressed as $\cos\theta$, giving

$$Z_r = \rho_0 c S \cos(\theta_a) e^{j\theta_a}$$

as listed in Eq. 6.4.

B.2 Webster Horn Equation

The Webster horn equation is a proper subset of the lossless telegrapher equations, with the added restriction that $C(x)L(x) = 1/c^2$, thus the wave speed is constant everywhere in the line. Like the telegrapher equations, the Webster horn equation can be properly expressed as two first-order partial differential equations:

$$\frac{\partial}{\partial x}\begin{bmatrix} v(x,t) \\ i(x,t) \end{bmatrix} = -\begin{bmatrix} 0 & L(x) \\ C(x) & 0 \end{bmatrix}\frac{\partial}{\partial t}\begin{bmatrix} v(x,t) \\ i(x,t) \end{bmatrix} \tag{B.1}$$

This formulation uses spatial voltage and current, whereas the acoustic formulation uses spatial pressure and volume velocity instead. Table B.1 shows the mapping between electrical and acoustical variables. Mass density ρ_0 and bulk modulus $\eta_0 P_0$ are used to model the per-unit-length inductance and capacitance, respectively. The spatial area $A(x)$ describes the area of the wave-front propagating in a symmetric waveguide. The speed of sound

Table B.1: Equivalent variables between electrical and acoustical formulation.

Electrical			Acoustical
Voltage	$v(x,t)$	$p(x,t)$	Pressure
Current	$i(x,t)$	$u(x,t)$	Volume velocity
Spatial inductance	$L(x)$	$\frac{\rho_0}{A(x)}$	Spatial mass density
Spatial capacitance	$C(x)$	$\frac{A(x)}{\eta_0 P_0}$	Spatial bulk modulus

in the medium is given as:

$$c = \sqrt{\frac{\eta_0 P_0}{\rho_0}} \tag{B.2}$$

where η_0 is the ratio of specific heats, P_0 is the equilibrium pressure, and ρ_0 is the spatial mass density.

The spherical radiator described in Section B.1 can be described exactly using Webster's horn equation (Putland, 1993) when $A(x) \propto x^2$.

B.3 Acoustic Capacitors

At low frequencies, the input impedance to a sealed cavity can be approximated using an ideal capacitor (Kinsler et al., 2000, p.287). At higher frequencies, the wave nature of the cavity becomes more prevalent, requiring a more precise wave model instead of lumped elements. A few example equal volume geometries, but with different $A(x)$, will be given.

Each of these examples is computed numerically, by means of segmenting the area function into small, uniform area cylinders, cascaded together. Section 4.6 shows the T-matrix used for cascading these finite-length transmission lines. The characteristic impedance of a uniform acoustic waveguide is given as:

$$Z_0 = \frac{\rho c}{A} \tag{B.3}$$

which is used in each T-matrix. The initial area for all geometries will be unity ($A(0) = 1$) and the total volume of these different geometries will be set to unity as well. Equal volumes and initial areas make the low-frequency compliance behavior comparable across different geometries.

Figure B.1 shows the cross-sectional radii ($\propto \sqrt{A}$) and the input impedance for five different geometries. The ideal capacitor has its first zero at $\omega = \infty$.

However, finite volume cavities allow for wave propagation, and thus standing waves are possible with nodes and anti-nodes located at the input causing poles and zeros in the impedance response, respectively.

The geometries are sorted by lowest-frequency initial zero, marked with colored circles along the base of Fig. B.1(b). Not surprisingly, as the geometry becomes shorter, the first zero increases in frequency. Smaller geometries permit standing waves at higher frequencies than do larger geometries when the wave speeds are identical.

B.4 Salmon Family of Horns

The area function used in Webster's horn equation has analytic solutions for certain geometries. One such set of geometries was described by Salmon and used hyperbolic trigonometric functions for defining the area function. This family of horns can be described by a single "Family Parameter" T, where "as T ranges from zero to infinity the horn contour changes from the hyperbolic cosine, through the exponential, and finially to the limiting conical horn" (Salmon, 1946). When $T = 1$, the family describes the exponential horn. When $T = \infty$, the family reduces to that of the simple conical horn. Several plots of the input impedance Z and reflectance $\mathcal{G}$ are shown in Fig. B.2. The solid lines denote the real component whereas the dashed lines denote the imaginary component.

When $T < \infty$, there exists a range of frequencies such that $|\mathcal{G}| = 1$; thus all the energy in this frequency range does not propagate; it is trapped in the horn. The reflectance chart, which for all intents and purposes is identical to a Smith chart, plots the real and imaginary components of $\mathcal{G}$ parametrically as a function of frequency. When this plot lies along the unit circle, the energy does not radiate because the system is purely reactive. The imaginary components for all these horns are non-negative, indicating an inductive load for the horn (See Section 6.2.1). At high frequencies, the reflectance for all these horns goes to zero, as all the energy radiates away at these frequencies.

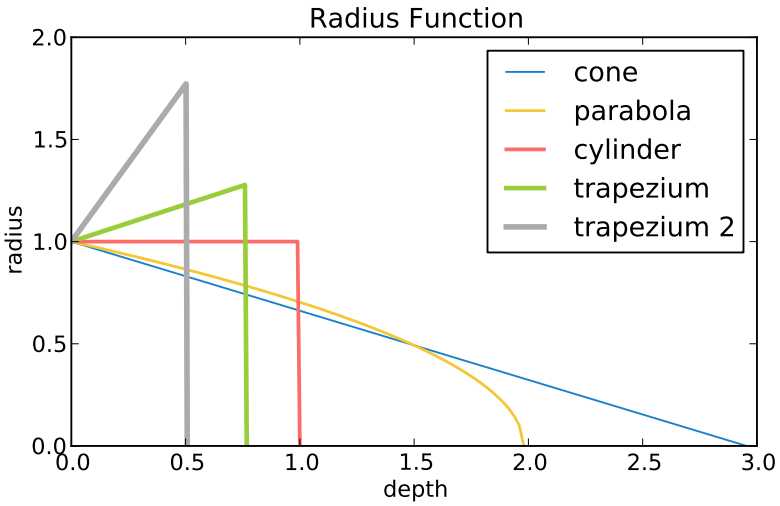

(a) Cross-sectional radii for equal-volume cavities

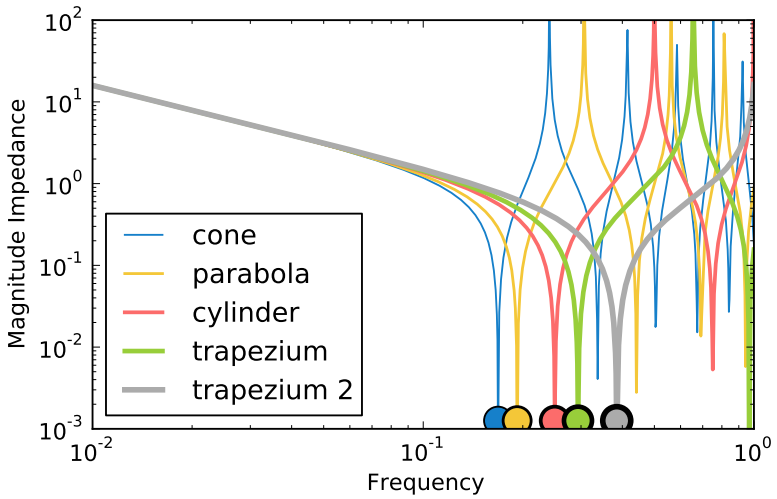

(b) Input impedance

Figure B.1: Radii and impedance of equi-volume cavities.

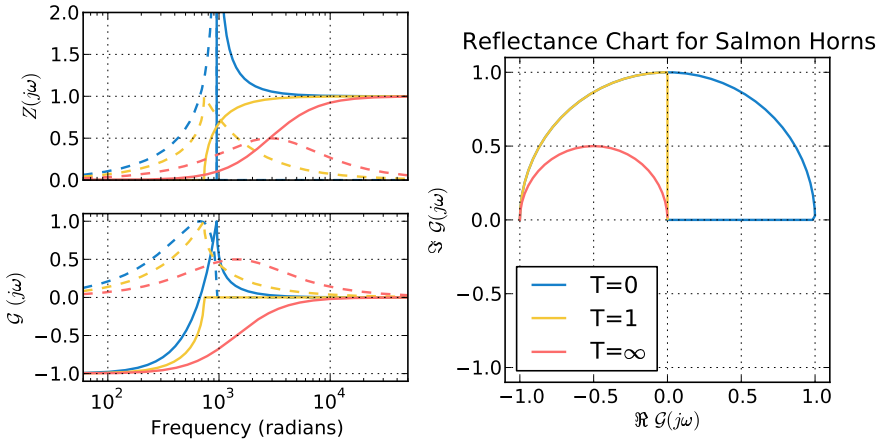

(a) Horns for $T \in \{0, 1, \infty\}$

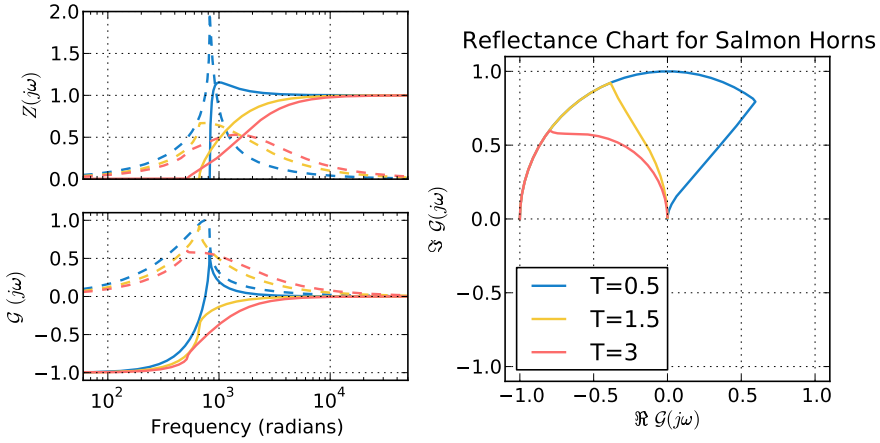

(b) Horns for $T \in \{0.5, 1.5, 3\}$

Figure B.2: Salmon family of horns. Real components of Z and $\mathcal{G}$ are solid lines; imaginary components are dashed lines.

REFERENCES

Arnold, D. N., & Rogness, J. (2008, November). Möbius transformations revealed. *Notices of the American Mathematical Society*, *55*(10), 1226-1231.

Belevitch, V. (1962, May). Summary of the history of circuit theory. *Proceedings of the IRE*, *50*(5), 848-855.

Boas, R. P. (1987). *Invitation to complex analysis*. New York: The Random House/Birkhäuser mathematics series.

Brune, O. (1931). *Synthesis of a finite two-terminal network whose driving-point impedance is a prescribed function of frequency*. Phd thesis, Massachusetts Institute of Technology, Cambridge, MA.

Caflisch, R. E. (1981). An inverse problem for Toeplitz matrices and the synthesis of discrete transmission lines. *Linear Algebra and its Applications*, *38*, 207-225.

Campbell, G. A., & Foster, R. M. (1942). *Fourier integrals for practical applications*. New York: Bell Telephone System Laboratories.

Fettweis, A. (1986). Wave digital filters: Theory and practice. *Proceedings of the IEEE*, *74*(2), 270 - 327.

Foster, R. M. (1924). A reactance theorem. *Bell System Technical Journal*, *3*, 259-267.

Greenberg, M. (1998). *Advanced engineering mathematics* (2nd ed.). Upper Saddle River, NJ: Prentice Hall.

Gustavsen, B., & Semlyen, A. (1999, Jul). Rational approximation of frequency domain responses by vector fitting. *Power Delivery, IEEE Transactions on*, *14*(3), 1052-1061.

Heaviside, O. (1950). *Electromagnetic theory* (Vol. 1-3). New York: Dover

Publications, Inc.

Johns, P. B., & O'Brien, M. (1980, Jan-Feb). Use of the transmission-line modelling (t.l.m.) method to solve non-linear lumped networks. *Radio and Electronic Engineer*, *50*(1.2), 59-70.

Kinsler, L., Frey, A., Coppens, A., & Sanders, J. (2000). *Fundamentals of acoustics*. Hoboken, NJ: John Wiley & Sons, Inc.

Lin, S., & Kuh, E. (1992, May). Padé approximation applied to lossy transmission line circuit simulation. In *Circuits and Systems, 1992. ISCAS '92. Proceedings., 1992 IEEE International Symposium on* (Vol. 1, p. 93-96).

Lundberg, K., Miller, H., & Trumper, R. (2007, Feb.). Initial conditions, generalized functions, and the Laplace transform troubles at the origin. *Control Systems, IEEE*, *27*(1), 22-35.

Lützen, J. (1979). Heaviside's operational calculus and the attempts to rigorise it. *Archive for History of Exact Sciences*, *21*, 161-200. (10.1007/BF00330405)

Montgomery, C. G., Dicke, R. H., & Purcell, E. M. (1948). *Principles of microwave circuits* (3rd ed., Vol. 8). McGraw-Hill Book Company, Inc.

Pai, M. A. (2003). *Power circuit and electromechanics*. Champaign, IL: Stipes Publishing LLC.

Parent, P., & Allen, J. B. (2007). Wave model of the cat tympanic membrane. *The Journal of the Acoustical Society of America*, *122*(2), 918-931.

Pillage, L. T., Rohrer, R. A., & Visweswariah, C. (1994). *Electronic circuit and system simulation methods*. TX: McGraw-Hill.

Press, W. H., Teukolsky, S. A., Vetterling, W. T., & Flannery, B. P. (2007). *Numerical recipes: The art of scientific computing* (3rd ed.). Cambridge, NY: Cambridge University Press.

Putland, G. R. (1993). Every one-parameter acoustic field obeys Webster's horn equation. *J. Audio Eng. Soc*, *41*(6), 435–451.

Rao, N. (2004). *Elements of engineering electromagnetics* (6th ed.). Upper Saddle River, NJ: Pearson Prentice Hall.

Salmon, V. (1946). A new family of horns. *The Journal of the Acoustical Society of America*, *17*(3), 212-218.

Sondhi, M. M., & Gopinath, B. (1971). Determination of vocal-tract shape from impulse response at the lips. *The Journal of the Acoustical Society of America*, *49*(6B), 1867-1873.

Tellegen, B. D. H. (1948). The gyrator, a new electric network element. *Philips Res. Rep.*, *3*, 81–101.

Valkenburg, M. E. V. (1955). *Network analysis*. Englewood Cliffs, NJ: Prentice-Hall.

Vanderkooy, J. (1989). A model of loudspeaker driver impedance incorporating eddy currents in the pole structure. *J. Audio Eng. Soc*, *37*(3), 119–128.

Weece, R., & Allen, J. (2010). A method for calibration of bone driver transducers to measure the mastoid impedance. *Hearing Research*, *263*(1-2), 216–223.

Yee, K. (1966, May). Numerical solution of initial boundary value problems involving maxwell's equations in isotropic media. *Antennas and Propagation, IEEE Transactions on*, *14*(3), 302 -307.